TALLINN UNIVERSITY OF TECHNOLOGY
School of Information Technologies

Tõnis Talviste

DETERMINATION AND ANALYSIS OF IGBT MODULE CURRENT SHARING TESTING LIMITS

Master's thesis

Supervisor: Indrek Roasto
PhD

Advisor: Joonas Leppänen
M.Sc.Tech.

Tallinn 2021

TALLINNA TEHNIKAÜLIKOOL
Infotehnoloogia teaduskond

Tõnis Talviste

IGBT MOODULI VOOLU JAGUNEMISE TESTIMIS-LIMIITIDE DETEKTEERIMINE JA ANALÜÜS

Magistritöö

Juhendaja: Indrek Roasto
Doktorikraad

Konsultant: Joonas Leppänen
Magistrikraad

Tallinn 2021

Author’s declaration of originality

I hereby certify that I am the sole author of this thesis. All the used materials, references to the literature and the work of other persons have been referred to. This thesis has not been presented for examination anywhere else.

Author: Tõnis Talviste

09.05.2021

Abstract

Determination and Analysis of IGBT Module Current Sharing Testing Limits

In their inverter unit, manufacturers are using IGBT modules in parallel to obtain higher current for the applied voltage. In total, three IGBT modules are used for the inverter unit and every IGBT module has three branches. Branch current deviation is tested with a double pulse tester. Current deviation limit is applied to determine if the IGBT module passes the test or fails. Limits that are in current use show numerous failures. The purpose of the thesis is to test failed modules and find out how high current deviation affects the inverter unit lifetime. This thesis is written in English and contains 62 pages, including 6 chapters, 52 figures and 3 tables.

Annotatsioon

IGBT mooduli voolu jagunemise testimis limiitide detekteerimine ja analüüs

Sagedusmuunduri tootjad kasutavad transistormooduleid paralleelahelas, et võimaldada sama pingeklassi juures suuremat voolutugevust. Ühes sagedusmuunduris kasutatakse kolme transistormoodulit, igas transistormoodulis on kolm poolsild vaheldit ning kõiki kolme korraga lülitatakse paralleelselt. Iga transistormoodulit testitakse lühiajalise vooluimpulssiga, millega saab võrrelda paralleelsete poolsild vaheldite voolutugevust. Hetkel kasutusel olevad testri limiidid ei ole teaduslikult testitud ning vajavad analüüsimist. Selle magistritöö põhieesmärk on uurida kas oleks võimalik tõsta voolujagunemise testri limiite ning selle võimalikku mõju sagedusmuunduri elueale. Lõputöö on kirjutatud inglise keeles ning sisaldab teksti 62 leheküljel, 6 peatükki, 52 joonist, 3 tabelit.

List of abbreviations and terms

IGBT	Insulated-gate bipolar transistors
FWD	Freewheeling diode
GDU	Gate drive unit
DBC	Direct bonded copper
ALT	Accelerated life test
NPT	Non-Punch Through
SPT	Soft Punch Through
PT	Punch Through
MOSFET	Metal–oxide–semiconductor field-effect transistor
DUT	Device under test
PCBA	Printed circuit board assembly
CSV	Comma - separated values
EmCon	Emitter based freewheeling diode
CAL	Carrier axial lifetime diode
SOA	Safe operating area
IEC	International Electrotechnical Commission
VCS	Voltage source inverter
PPI	Press-Pack IGBT
TIM	Thermal interface material
IEEE	Institute of Electrical and Electronics Engineers

List of symbols

V_{ce}	IGBT Collector emitter voltage
V_f	FWD forward voltage
r_{ce0}	IGBT on-state resistance
r_{f0}	FWD on-state resistance
I_c	Collector current
I_f	Forward current
T_j	Junction temperature
T_{jc}	Junction to case temperature
T_c	Case temperature
T_{ch}	Case to heatsink temperature
R_{tha}	Thermal resistance of the heatsink
R_{thjc}	Thermal resistance junction to case
R_{thch}	Thermal resistance case to heatsink
T_H	Heatsink temperature
P_{cond}	Conduction loss
P_{sw}	Switching loss
E_{ON}	Turn-on energy
E_{OFF}	Turn-off energy
f_{sw}	Switching frequency

Table of contents

List of figures

List of tables

1 Introduction

Today's power converters need high power density from a single inverter unit specially for energy harvesting and traction industry. For 1700 V insulated-gate bipolar transistor (IGBT) modules, there are only few options for over 1000 A current rating [1]. To acquire more power from the inverter unit, a 6-pack IGBT module is used as a 2-pack module by paralleling phase legs of 6-pack IGBTs and freewheeling diodes (FWD). Paralleling more than two phase legs is a complicated task for ensuring equal current share. The highest current levels that can be achieved by paralleling IGBTs and FWDs may be around 5 kA and more [2]. Three phase leg IGBT/FWD modules are used in parallel to achieve maximum selected current. This type of switching needs complicated gate driving logic and accurate IGBT/FWD chip characteristics. Every phase of the IGBT/FWD chip in the module should consume the same amount of current. There are variations between different IGBTs and FWDs caused by silicon wafer resistivity, front-end – chip processes and back-end – bond wires. Currently, IGBT/FWD suppliers are not willing to limit the variation in the current sharing of the 6-pack mode; thus, the inverter manufacturers are sorting these modules by additional current sharing test in their production. This is tested with a pulse tester, which modulates current through every IGBT/FWD phase leg and then compares the average current values in static and dynamic states. Current deviation specification limits were developed for older generation IGBT modules and were then transferred to new generation IGBT modules. Due to the high rate of failures with the new generation IGBT/FWD, it is required to study if it is possible to increase current deviation limits. Chapter 2 addresses the IGBT and operation principle, researching state of the art technology. In Chapter 3, paralleling of the IGBT/FWD module and current sharing will be investigated. Chapter 4 explains the testing of the 2-pack module in the static and dynamic aspects. Starting from Chapter 5, the possibility to raise the current deviation limits will be analyzed. I am calculating IGBT and FWD junction temperature values with different current deviation modules. With those values the IGBT/FWD theoretical junction temperature is obtained and the results are compared. After theoretical analysis, accelerated life testing (ALT) with different characteristics of IGBT and FWD will be conducted. Using the results of the accelerated life testing enables the estimation of possible lifetime for IGBT and FWD chips and the final decision if the current deviation limits can be raised or not.

2 IGBT and FWD

This chapter addresses the IGBT and FWD operation principle. I will share information for different IGBT packaging types. The last part in this chapter focuses on the cycle lifetime of the IGBT/FWD module because 20% of power converter failures come from IGBT/FWD [3].

2.1 IGBT operation principle

IGBT is a transistor that combines benefits of the bipolar transistor and the metal oxide semiconductor field effect transistor (MOSFET). Bipolar transistor voltage drop at turn-on is much lower than that of MOSFET at comparable current and blocking voltage. MOSFET consumes less gate energy for turning on than a bipolar transistor. Figure 1 shows IGBT structured layer and equivalent circuit.

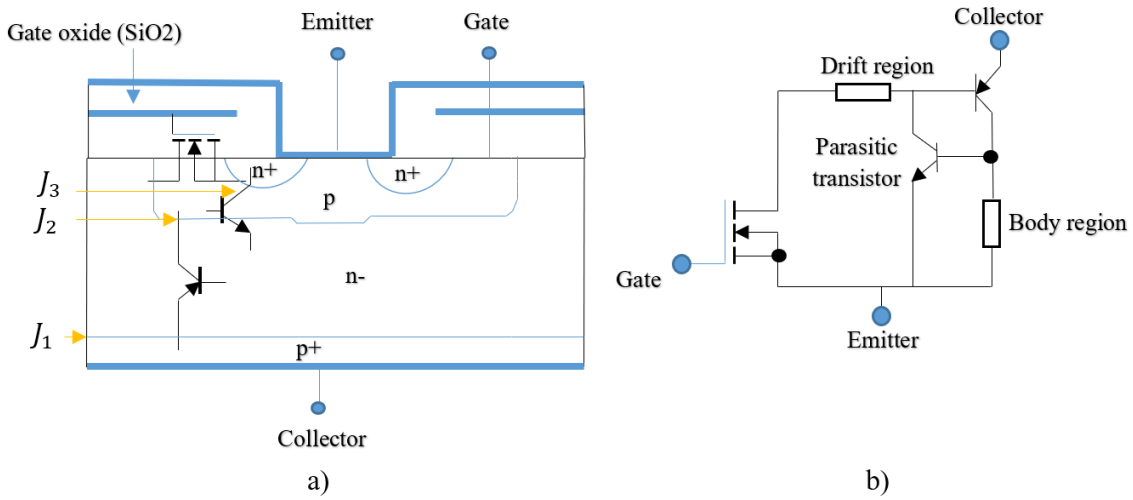

Figure 1 a) IGBT layer model; b) Equivalent circuit with internal parasitic thyristor structure [2].

IGBT is structured similar to vertical MOSFET except it has p^+-doped zone called a collector. There are three pn-junctions - J_1, J_2, J_3 from which J_2 is blocking and J_1 and J_3 are conducting. If the IGBT is turned off, there is 0V or negative voltage on the gate and the emitter is more negative than the collector. When positive voltage is applied to the gate (usually 15 V), then IGBT turns on and changes to the forward conduction mode. First conduction channel is applied at p-region, also called body region at equivalent circuit Figure 1 b), which moves electrons from the emitter to the n^- doped area called a drift region, as shown in Figure 1 b) equivalent circuit. It is reducing the potential of n^-

base and opens pn-junctions at J1. Minority carriers are moving from p^+-doped to n^- base, which changes concentration of minority carriers of several magnitude. For charge neutrality, electrons must flow from the emitter to the n^- base. The process when a charge carries a flow from the n^+ region to the relatively high impedance n^- base region is called conductance modulation [2].

It also reduces sharply the voltage drop across the collector-emitter path of the IGBT. As compared to MOSFET, the conduction losses are smaller, especially at higher currents [2]. Figure 2 shows the output characteristics of IGBT for different gate emitter voltages.

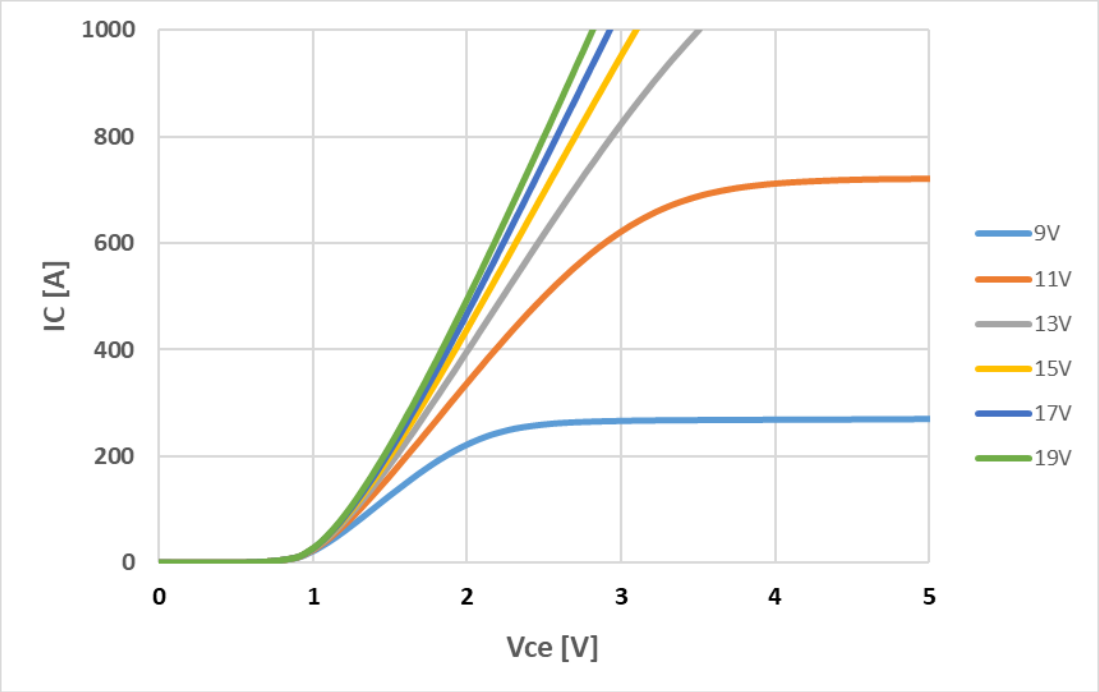

Figure 2 Example of one specific IGBT characteristics with different V_{ge}.

If the gate voltage is insufficient, then the inversion layer formed is weak and the number of electrons that flow into the drift zone is smaller. Voltage drop via IGBT increases and the IGBT reaches the active area. When the IGBT is conducting in the active area, significant losses could destroy it [2].

When the gate-emitter voltage is turned 0V, then the gate channel re-forms, preventing electrons to come into the drift zone. Because of high concentration of charge carriers at the drift zone, the electrons are flowing into the p^+ doped collector layerand the holes are following them. Remaining charge carriers must be removed by recombination. Turn-off IGBT current can be added in two phases – the first phase is turning off the inversion layer, which causes rapid current decreases and the second phase is recombination of charge carriers, which gives long tail current. This tail current causes higher turn-off losses than MOSFET [2].

IGBT technology has been developing during the years and several changes have been made in the design regarding doping profiles. Punch through (PT) profile shown in Figure 3 a) was the first IGBT available from low- to medium-power range with voltages up to 1200 V [4]. It had heavy lifetime reduction necessary due to the strong and thick p+ anode substrate. PT IGBT suffered from strong negative temperature coefficient during on-state and snappy turn-off switching behavior due to the short lifetime in the base region; because of those factors, PT IGBT cannot be used in parallel applications [4]. Non-punch through (NPT) technology shown in Figure 3 b) was the solution for the paralleling because it had very weak anode and therefore no lifetime engineering was necessary. NPT had positive temperature coefficient, short circuit ruggedness but high turn-on and turn-off losses [4].

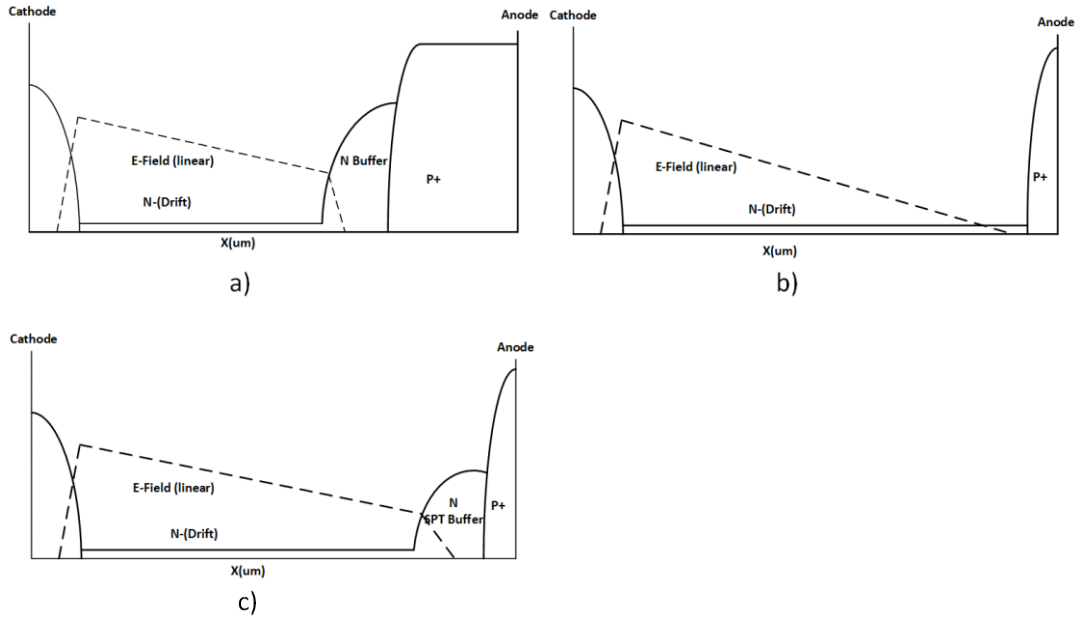

Figure 3 Doping profiles and electrical field distribution for a) punch through doping profile; b) non-punch through doping profile and c) soft punch through doping profile [4].

A solution for this problem would be soft punch through (SPT) IGBT technology shown in Figure 3 c), which matches the NPT performance and low switching losses from the SPT structure. SPT has a weak anode similar to NPT but with optimized low-doped deep n-buffer. SPT buffer will give field penetration during the blocking state, still allowing good conductivity during on-state [4].

There are several possibilities for IGBT cell design, as shown in Figure 4.

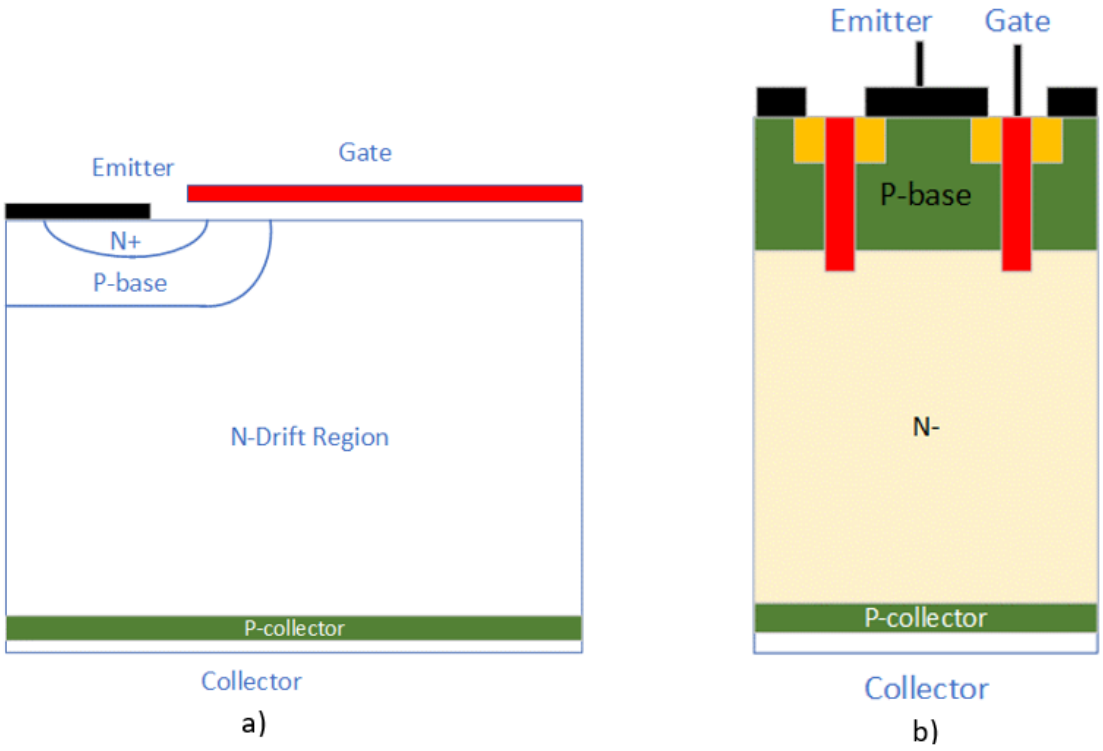

Figure 4 NPT IGBT cell cross-section: a) planar; b) trench [5].

Trench cell design in Figure 4 b) is an improved version of the planar design in Figure 4 a) and its main benefits are smaller design, which means that cell density can be much higher. Increased density gives higher currents with lower collector emitter voltage.

2.2 FWD operation principle

Diode is an electrical device that works on the pn-junction principle. Diodes are forward conducting electrical devices. Simple p-n junction is described in Figure 5.

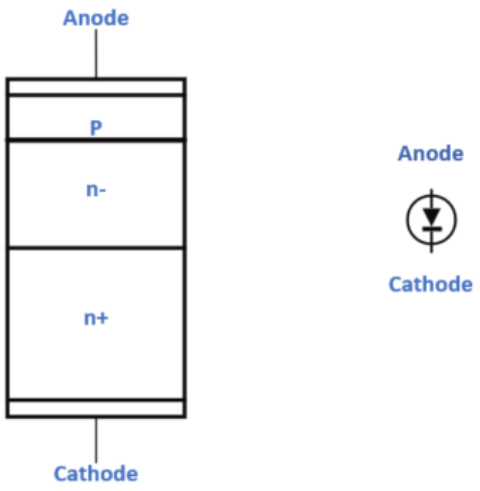

Figure 5 Diode layer module and symbol [2].

The electrode that is connected to the diode p-zone is called an anode and the electrode that is connected to the n-zone is called a cathode. At forward conducting, current is nearly zero until the threshold voltage is achieved and after that current is rising exponentially with increasing forward voltage, as shown in Figure 6.

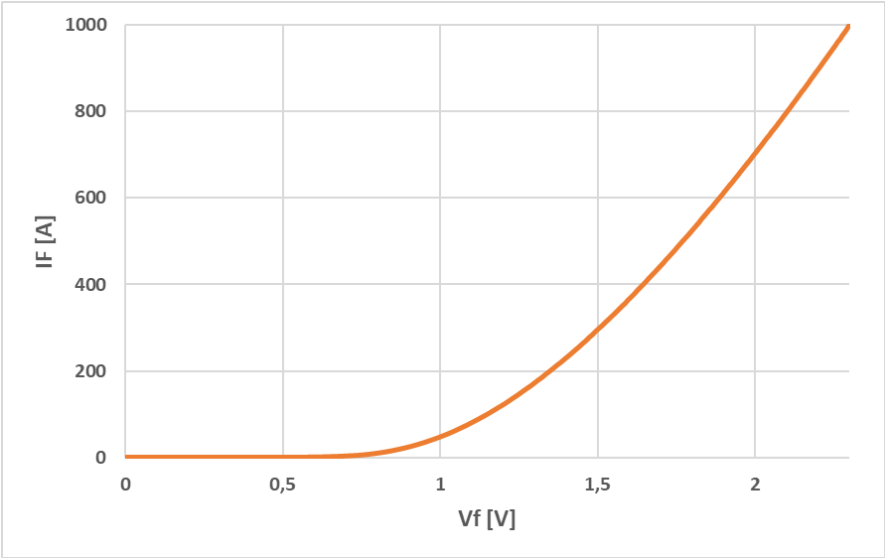

Figure 6 Example of one specific FWD I-V characteristic.

At the reverse direction, the diode will consume very low power until breakdown voltage, which leads to thermal breakthrough and eventually destroying the component [2].

In the IGBT module, fast recovery diodes, also called freewheeling diodes (FWD), are used. These suit for high frequency applications and are used in conjunction with a controllable power semiconductor. Their reverse recovery time is very low, up to a few microseconds. Reverse recovery time makes reference to how fast a diode can turn from the conducting state to the blocking state with its stationary reverse current value [2]. For a freewheeling diode, emitter based (EmCon) technology or controlled axial lifetime (CAL) technology are used. Concentration profiles of both diode technologies are shown in Figure 7. CAL diode has much deeper and stronger anode p+ region with local lifetime control area than the EmCon diode, which is emitter-based concept with low doped anode region without local lifetime control [4].

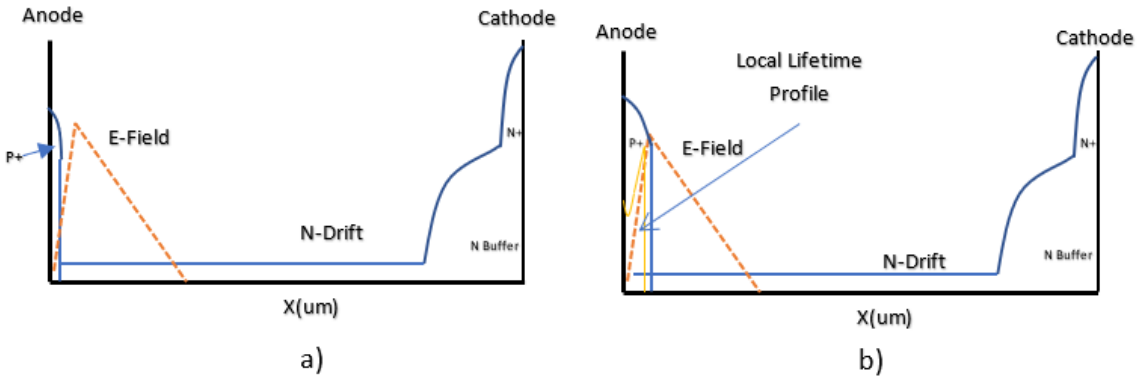

Figure 7 Concentration profiles for a) EmCon diode; b) CAL diode [4].

CAL diodes provide very good surge current capability and safe operation area (SOA) performance, but they have higher leakage current due to the local lifetime control [4]. EmCon diodes, on the other hand, provide low leakage current due to the absence of the local lifetime control, but their drawbacks are bad surge current capability and SOA performance [4].

2.3 Module construction

In the previous part, IGBT and FWD were described at the physics level. Next, the focus will be on how single and multiple transistor chips are packed. Transistors could be packed in several ways, as shown in Figure 8. A discrete device consists of a single IGBT and the most popular package type is TO-220. This type of package is a popular choice for mounting IGBT directly on the printed circuit board assembly (PCBA) [6].

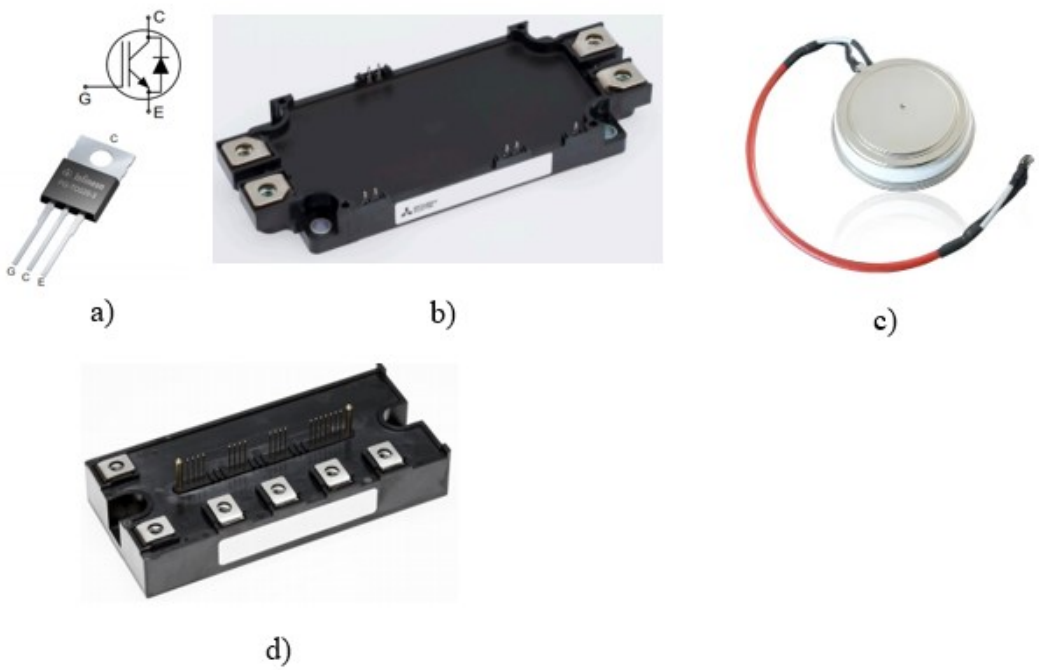

Figure 8 IGBT package types: a) Discrete device package TO-220; b) Power module; c) Disc type press-pack module and d) Smart Power module [7] - [10].

The next type would be a basic power module, which is the main object in this thesis. Power module layers are shown in Figure 9.

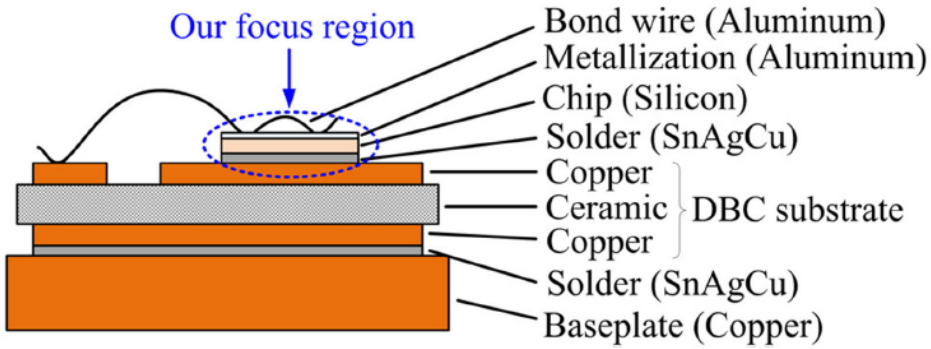

Figure 9 IGBT module layers [11].

On top are bond wires, which connect different chips together. To achieve higher current IGBT modules, multiple chips must be connected in parallel since the modern IGBT technology is limited to 200 A current per chip [2]. Parallel chips are shown in Figure 10. To improve humidity and mechanical robustness against dust, silicon chips and bond wires are covered with soft silicon gel [12].

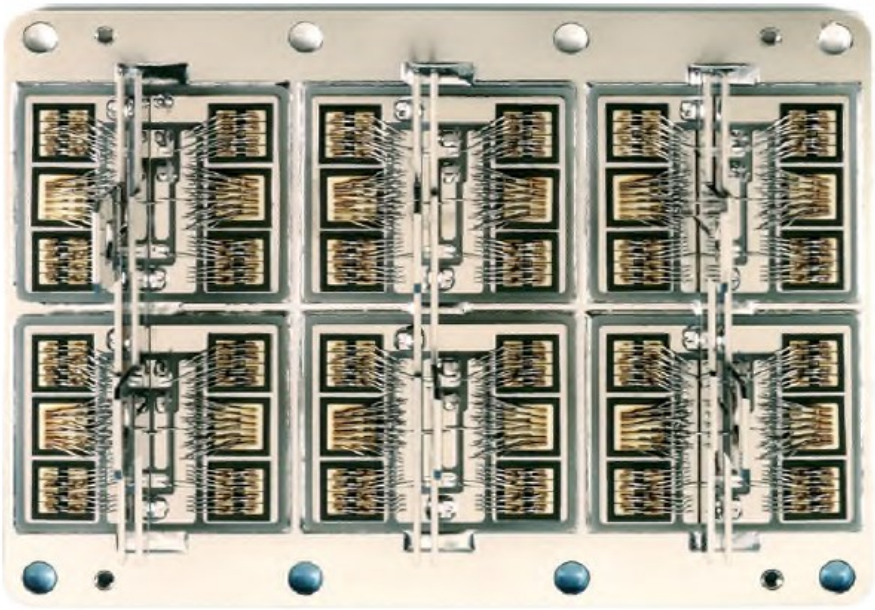

Figure 10 IGBT chips in parallel [13].

Silicon chips are soldered into a patterned copper plate, which together with ceramic form a direct bonded copper substrate (DBC) for cooling down the chips themselves. Ceramic is added as electrical isolation, providing good low thermal resistance. DBC is soldered onto the baseplate but there are variants of IGBTs where DBC is connected directly to heatsink [14]. Heatsink is usually made from aluminium and IGBT is added onto heatsink with a thermal interface material. Thermal interface material (TIM) is needed for decreasing thermal coupling between the IGBT module and heatsink. TIM can be thermal grease [15] or for example, graphite sheet [16]. Graphite sheet will have longer lifetime compared to thermal grease because overtime thermal grease will be pumped out [16].

Press-Pack power module is an enhanced version of the power pack module. This module is used in voltage source inverters (VCS) for power system applications, e.g., in high voltage direct current transmission lines [17]. Press-Pack IGBT(PPI) can consist of several IGBT chip-stacks, up to 36pc according to [17]. There are several advantages over power module IGBT. For example, PPI does not have bonding wire and solder layers and therefore, it is more robust at power and thermal cycling. It has been verified that PPI has much longer lifetime at the accelerated life test [18]. Downside of the PPI is that it has mechanically complex assembly [19].

Smart power modules will be the next generation device, enabling high power management together with control of switching, protection of over-current and over-voltage. The idea is to pack IGBT chips and diodes with controlling circuits in the same

package. That kind of approach is very attractive to lower power home electronics devices [6].

2.4 Cycle lifetime

It has been proven that the lifetime of the IGBT module depends on the wire bonds of the top of the chips and the robustness of the solder joint between the direct bonded copper substrate (DBC) and the baseplate [20]. There are different thermal cycling types for testing IGBT reliability, as shown in Figure 11.

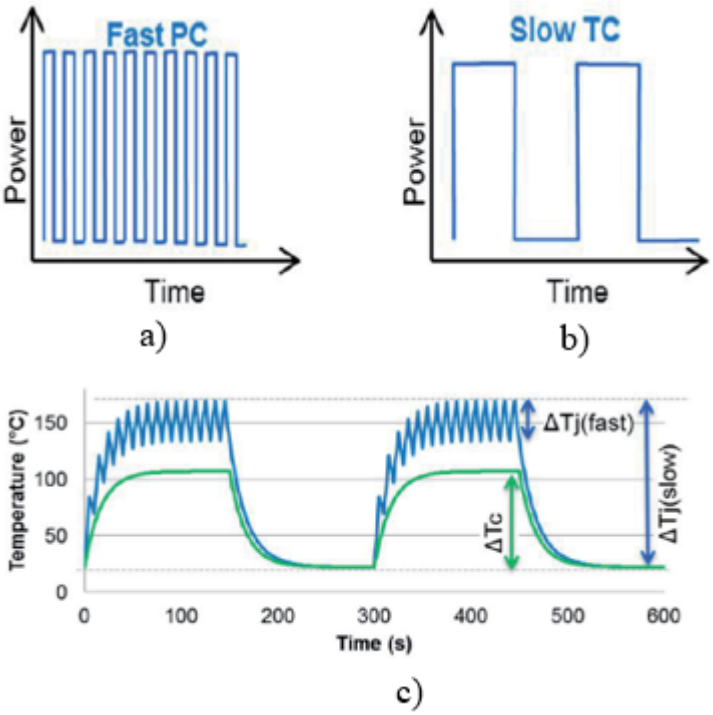

Figure 11 a) Power cycling; b) thermal cycling; c) power cycling plus thermal cycling [21].

At thermal cycling, the main failures occur between the DBC substrate and the baseplate and main indication is the rise of the IGBT/FWD case temperature (ΔT_c). Power cycling will have effect on bond wire cracks and the solder joint between the die and the DBC substrate and the main indication is IGBT/FWD junction temperature (ΔT_j) [3].

Figure 12 shows the copper baseplate with different thermal cycling times. The higher the cycling time, the more the copper will crack and wear out. This will deteriorate the thermal heat path and the operation temperature will rise over the years.

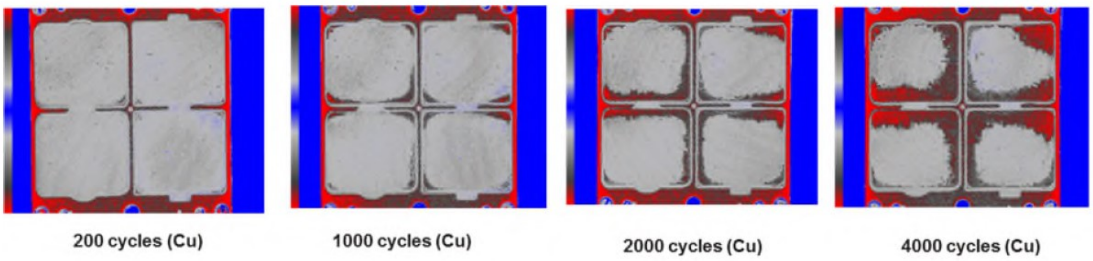

Figure 12 IGBT baseplate copper with different thermal cycling [13].

Typical crack of the solder layer between the DBC substrate and the copper baseplate can be seen from the cross-section joint after thermal cycling, as shown in Figure 13.

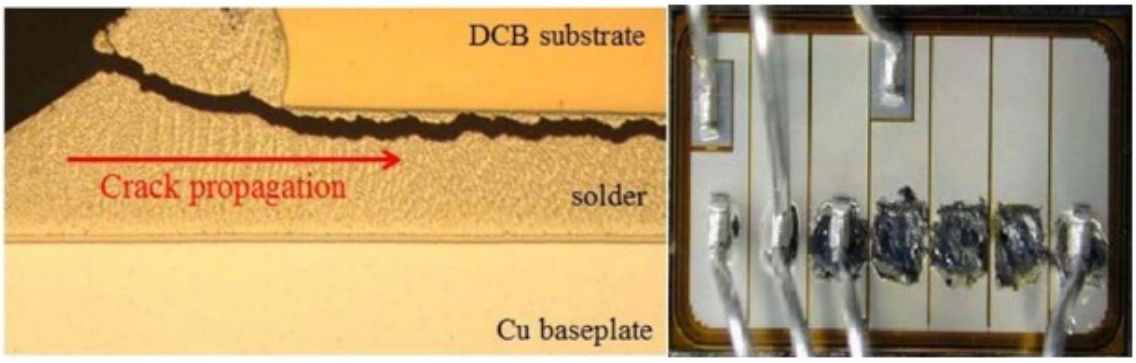

Figure 13 Solder layer crack between the DBC substrate, the Cu baseplate [3] and bond wire lift-off [22].

According to the literature, there are different ways of improving solder layer strengthening by changing the consistence of the solder alloy [3] for IGBTs, the junction temperature of which goes up to 175 °C. Inside the IGBT module, there are many bond wires that connect several micro-chips together, as shown in Figure 10. Over time, those bond wires will lift off because of the thermal expansion coefficient mismatch between the bond wire and the IGBT die. The difference of the thermal coefficient is the largest under power cycling thermal stress. An example of bond wire lift-off is shown in Figure 13. Bond wire life expectance will depend on the bond wire material and location from the die.

3 Current sharing in parallel IGBTs

Current sharing in parallel IGBT and FWD can be tested in two ways: static state and dynamic state. At the static state, IGBT/FWD is switched constantly ON, which means that steady current flows through the device. At the dynamic state, IGBT is switched ON and OFF with many cycles and FWD is used for reducing high voltage transient generated by the inductance. Mainly at the static state, IGBT collector emitter voltage and FWD forward voltage have variations between different manufacturing lots because of resistivity of the wafer. At the dynamic state, main influencers are gate drive topology and stray inductance in busbars.

3.1 Static current sharing

When the parallel IGBTs are conducting, the same collector emitter voltage will be applied to all branches. Parallel IGBTs will have different collector current because of IGBT difference of on-state resistance and threshold voltage difference. On-state resistance variations come mainly in raw silicon wafer resistivity and semiconductor manufacturing process. The key for solving this problem would be choosing similar production date IGBTs to rule out collector emitter voltage differences. Equivalent circuit for IGBT is shown in Figure 14.

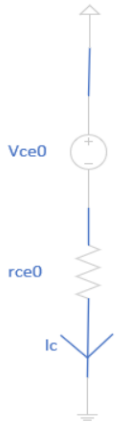

Figure 14 IGBT equivalent circuit in steady state condition [23].

Collector emitter voltage equals threshold voltage summed with collector current multiplied with on-state resistance, expressed by Eq. (1) [24]:

$$V_{CE}(I_C) = V_{ce0} + I_C * (r_{CE0} + R_{CC+EE}), \quad (1)$$

where $V_{CE}(I_C)$ is the collector emitter voltage, I_C is the collector current, r_{CE0} is the on-state resistance and R_{CC+EE} - module lead resistance.

The same approach can be used for describing FWD equivalent circuit in Eq. (2) [24]:

$$V_F(I_F) = V_{f0} + I_f * (r_{f0} + R_{CC+EE}), \quad (2)$$

where $V_f(I_f)$ is the FWD forward voltage, I_f - the forward current, r_{f0} - the on-state resistance and R_{CC+EE} - the module lead resistance.

Today, IGBTs are manufactured with trench gate field stop technology, which means that the collector emitter voltage increases with temperature. This means that if one module runs at 25 °C and the other at 125 °C, the cooler module will take most of the current share but eventually it will stabilize because higher current increases the temperature, as shown in a) Figure 15. Unfortunately, it is not the same for FWD because diode chips will have negative temperature coefficient, as shown in b) Figure 15. For FWD, it is crucial to choose chips from the same production lot for decreasing the current share in the applications, in particular, if the inverter unit also works as a rectifier.

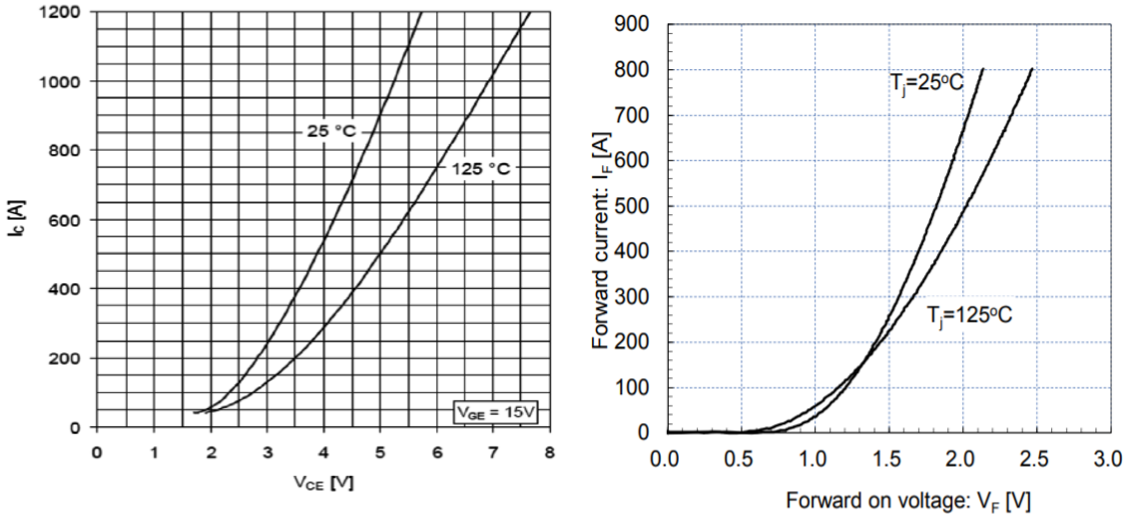

a) b)

Figure 15 a) Collector emitter voltage; b) FWD forward voltage at 25 °C and 125 °C [23], [25].

If the IGBT modules run in parallel, it is required to understand how much collector current each branch will get (Figure 16).

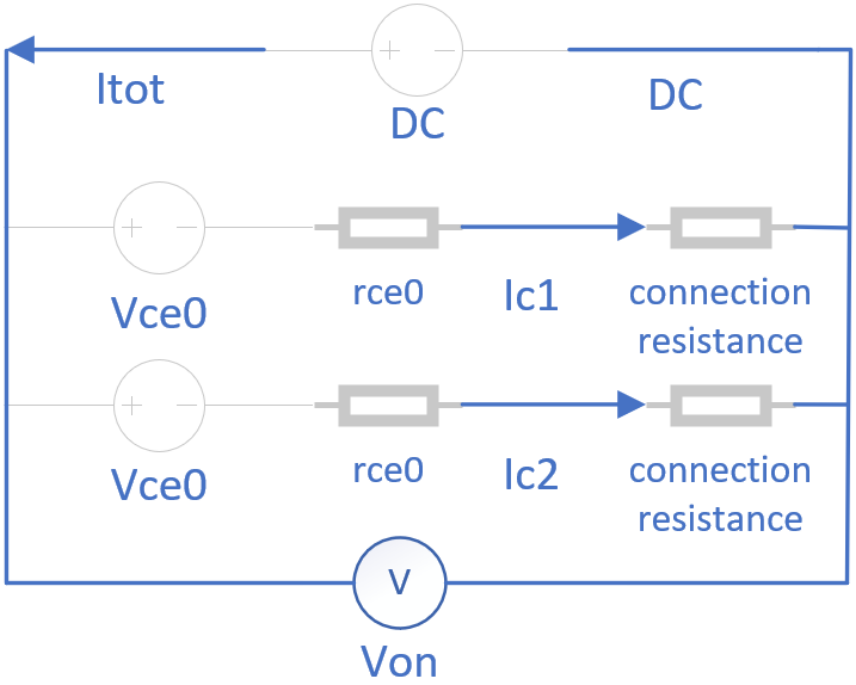

Figure 16 Parallel current sharing in the IGBT [23].

For calculating the collector current I_{c1} and I_{C2}, I can use Eq. (1) and simply calculate average collector emitter voltage for different IGBT chips in Eq. (3) [23]:

$$Ic_{(n)} = \frac{\frac{V_{ce(1)}+V_{ce(2)}+V_{ce(3)}}{3} - v_{ce0(n)}}{r_{ce0(n)}} \tag{3}$$

Parameters were described in Eq. (1).

The same equation can be used also for finding parallel FWD currents by Eq. (4) [23]:

$$If_{(n)} = \frac{\frac{V_{f(1)}+V_{f(2)}+V_{f(3)}}{3} - v_{f0(n)}}{r_{f(n)}} \tag{4}$$

Parameters of the equation were described in Eqs. (1) and (2).

3.2 Dynamic current sharing

3.2.1 Gate driver topology

Gate driver has minor influence on static current sharing because only the peak value of the gate emitter value will have effect; however, if the gate voltage variation is not well controlled by the manufacture, it could have higher influence. For dynamic current sharing, the gate driver plays more crucial role because it affects turn-on and turn-off times, which can cause mismatches. There are several possibilities to drive parallel IGBTs: common gate driver – where the same gate drive unit (GDU) will drive all

transistors; common gate driver with common mode chokes in the gate-emitter connection for decoupling the auxiliary emitter or with individual drivers. Figure 17 shows the direct drive gate driver in parallel circuits.

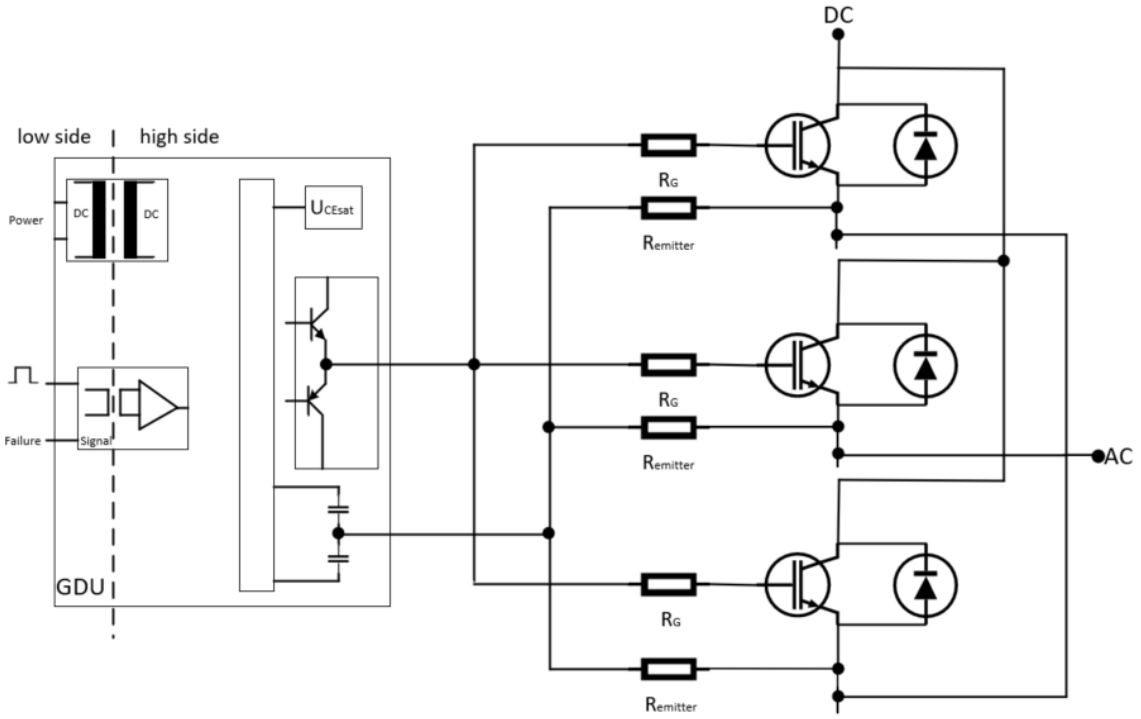

Figure 17 Direct gate drive in parallel connection [2].

Gate driver signal and power supply are galvanically isolated. The switching command comes from the central gate driver unit. A powerful output stage is required there because only one gate driver is used for all parallel transistors. Every gate has its own gate resistor for adjusting the switching behavior. Emitter resistor is the key element in the common gate drive for not damaging the IGBT module. Variation in the collector emitter threshold voltage, busbar stray inductance, ohmic and inductive tolerances in the gate path will cause dynamic peak currents. Emitter resistors are devices that absorb those dynamic peak currents which may exceed several hundred amps [2].

A disadvantage of the common gate drive is that there is no symmetrical current flowing between the emitter resistors. Two parallel IGBTs during turn-on and turn- off will cause different direction compensating currents; thus, it will give positive potential in one emitter resistor and negative voltage drop on the other emitter resistor [2]. For decreasing such kind of events, emitter resistors can be replaced with common mode chokes, as shown in Figure 18.

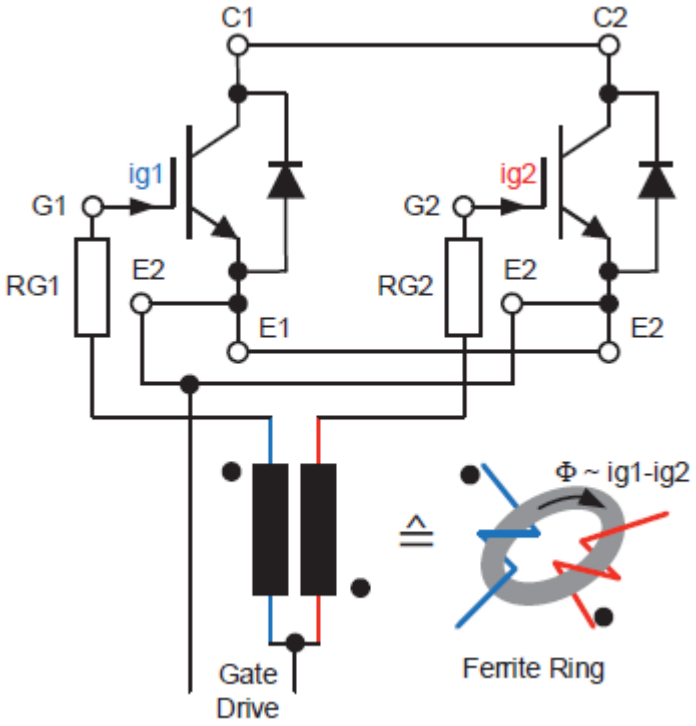

Figure 18 Common mode choke [26].

When different compensated currents are flowing into the gate and auxiliary emitter wires, common mode choke with its magnetic resistance can reduce that [2].

Another way for avoiding loop currents will be using an individual gate driver for every transistor gate. A disadvantage of using an individual gate drive is that different gate voltages and timing will affect current sharing because all drivers will suffer parameters variations [23].

3.2.2 Mechanical design - stray inductance

In parallel applications there is a need of re-thinking the mechanical design for reducing unwanted stray inductance in the circuit. Figure 19 a) shows that wire harness is connected at one side of the IGBT busbar. From the graph it can be seen that the phases are not equal. The IGBT that has the longest current path to the output will have the highest inductance and the IGBT that is the closest has the smallest inductance [27].

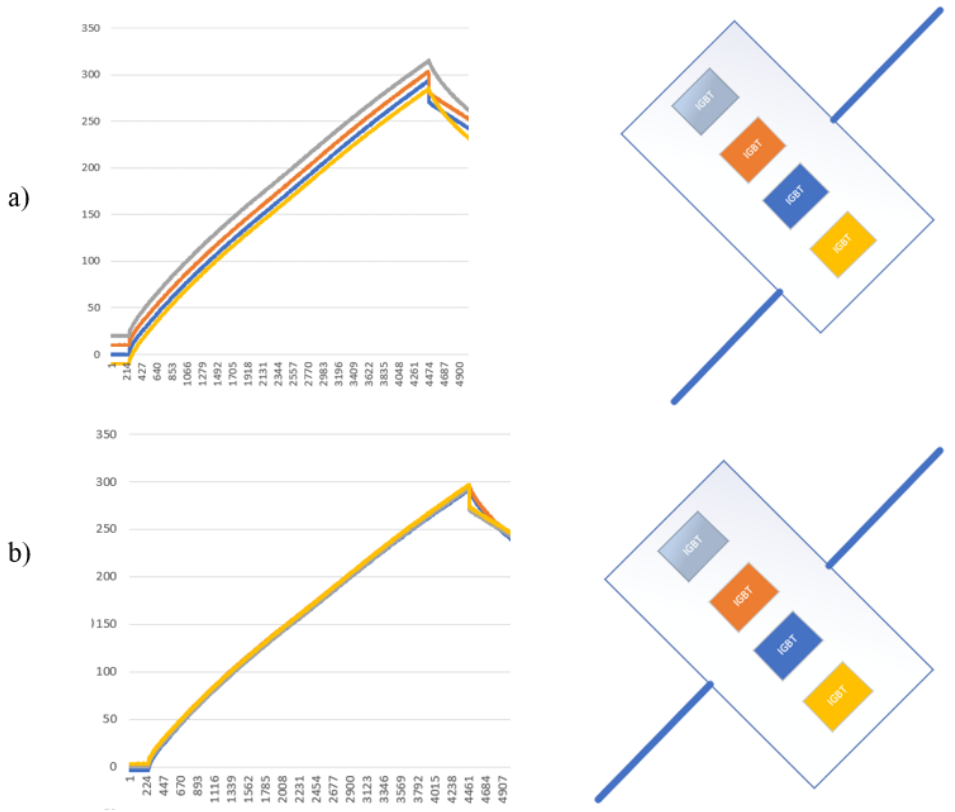

Figure 19 a) Stray inductance during IGBT turn – on; b) No stray inductance during IGBT turn - on [27].

Figure 19 b) shows that the output wire harness is connected in the centre of the IGBT busbar and there is no inductance difference between the IGBTs. As can be seen on the graph, all the phases have similar current share during IGBT turn–on [27].

If the output wire harness is routed in parallel with the IGBT busbar, there is current difference, as shown in Figure 20 Stray inductance by routing cable [27]. Output wire harness will affect IGBT busbars by the current that is flowing in different sides [27].

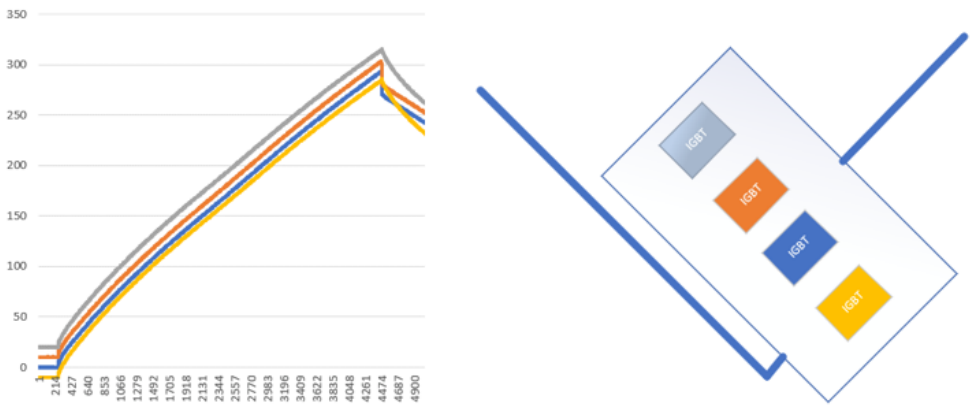

Figure 20 Stray inductance by routing cable [27].

Figure 21 shows an equivalent circuit of the above picture. If the AC wire harness is close to the AC busbar, there will be coupling between the two inductance $L\sigma 12$ and $L'\sigma 12$, as can be seen in the equivalent circuit, which basically is the voltage source with the terminal voltage $M_1 * \frac{di_{Load}}{dt}$. If the current changes overtime from $L'_{\sigma 12}$, it induces the voltage along the AC busbar due to the inductive coupling. Caused by this voltage, a circular current I_{12} flows counter clockwise through the network consisting of $L_{\sigma 1,} R_1$ and $L_{\sigma 2}, R_2$. The circular current with the load currents leads to the current distribution shown on the graph above [27].

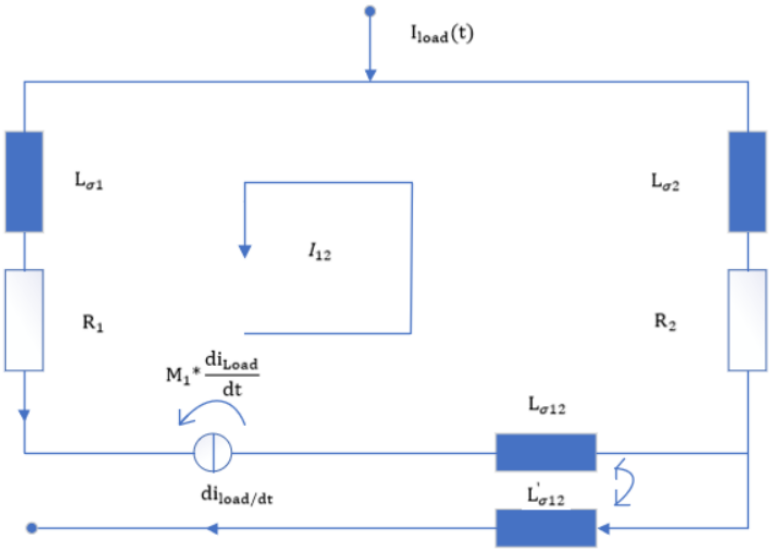

Figure 21 Equivalent circuit of stray inductance [27].

4 Paralleling 6-pack IGBT branches to 2-pack configuration

This chapter focuses on the testing of IGBT/FWD static and dynamic parameters from 6-pack mode to 2-pack mode. Both testing methods have different approaches for IGBT and FWD characterisation. When testing static parameters, constant current testing of only one pulse should be used. In dynamic testing, multiple pulses should be looked at to see IGBT turn-on and turn-off performance.

4.1 Testing static current sharing

With static current sharing, mainly IGBT I-V curves are studied. The emitter collector voltage (V_{ce}) and the diode forward voltage (V_f) difference with the constant collector current (I_c) is measured. For verifying that kind of test methods, I checked the IEC IGBT standard [28]. Figure 22 shows the circuit for measuring IGBT saturation voltage (V_{CEsat}). V_{GG} is the gate voltage source, V_{CC} with combination with R_1 provides constant collector current pulses. IGBT as the device under test (DUT) is in the centre. V_{CE} and i_C measurement points are marked in the circuit [28].

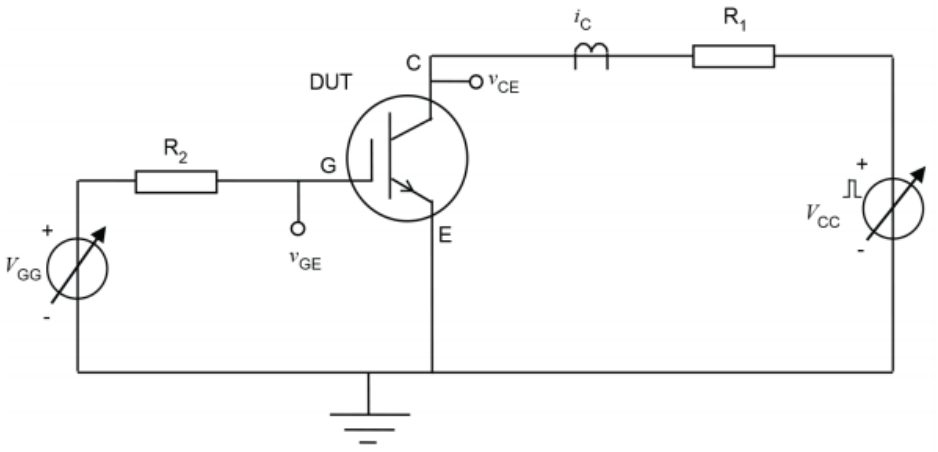

Figure 22 IEC standard circuit for measuring V_{ce} saturation [28].

In the FWD forward voltage measurement, I checked with the IEC standard measurement for a rectifying diode. There are three types of measurement according to the standard: DC method, AC method and using the pulse method [29]. Pulse method circuit is shown in Figure 23. Pulse widths should be such that internal heating is negligible, usually between 50 to 500 us. From the circuit, D would be DUT, G is pulse generator, R_1 is protective resistor and R_2 is calibrated current sensing resistor. Oscilloscope was used for

measuring forward voltage. Specified forward current is regulated by increasing the voltage of the pulse generator [29].

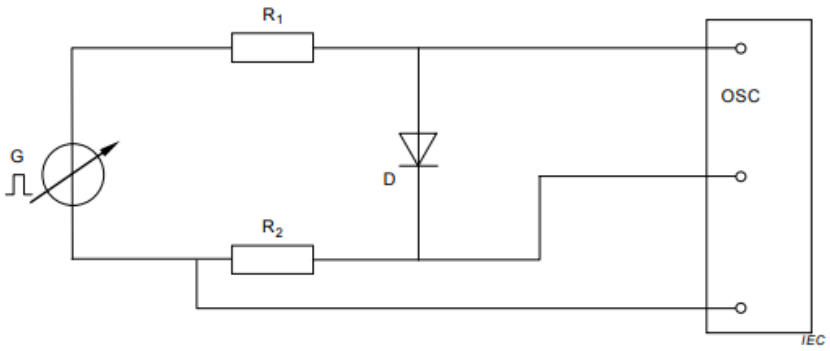

Figure 23 IEC standard for measuring the diode V_f [29].

For measuring the collector emitter voltage and the diode forward voltage, curve tracers are used. Curve tracers are devices used to measure the semiconductor IV curve, as shown in Figures 2 and 6. Nowadays curve tracers have many more functions, not just measuring the IC curve, e.g., an LCR meter, dynamic tester oscilloscope/PG, power loss calculation, automatic thermal test and many other functions [30].

Typically, the measurement circuits of a commercial curve tracer are classified. Thus, I was searching for a curve tracer developed by a researcher for free use. From the IEEE publications, I found a technical article addressing a Labview based curve tracer [31] for use by everyone. This curve tracer enables use of pulse measurement instead of very long static current to avoid transistor temperature rise under test. Two kinds of pulse methods are available: the drain-pulse method and the gate-pulse method, as shown in Figure 24 [31]. The drain-pulse method has a current switch on the drain terminal and the gate-pulse method has a current switch on the gate terminal. The gate-pulse method is easier to construct but the waveform of the input pulse is limited by the output voltage specification of the gate drive circuit. The drain-pulse method accepts any gate voltages to the transistor and the whole I-V range is covered [31].

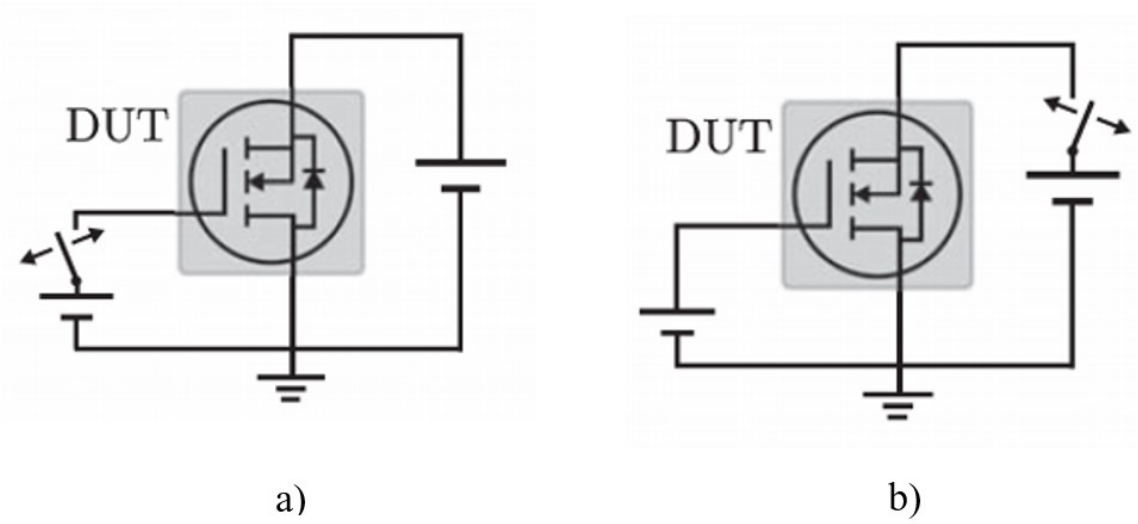

Figure 24 a) Gate-pulse method and b) drain-pulse method [31].

An example of the curve tracer circuit shown in Figure 25 was taken from the IEEE article [31]. It describes the drain-pulse method. Voltage and currents are monitored through the digital oscilloscope.

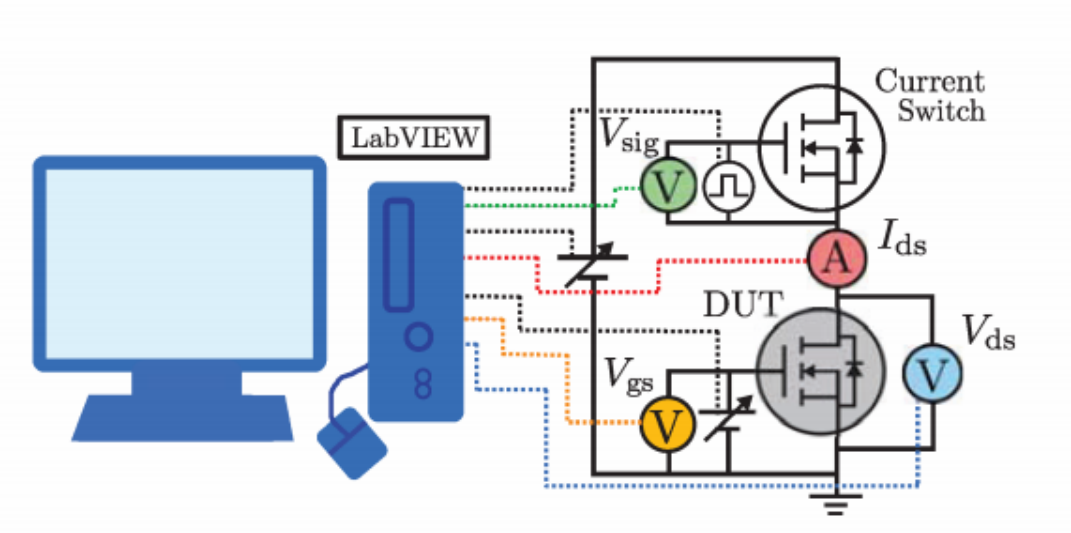

Figure 25 Curve tracer by the drain-pulse method [31].

Digital oscilloscope acts as a voltmeter for the gate and the drain-source voltage. Drain current is measured with an ammeter, which is usually a shunt resistor. All the data is combined in the digital oscilloscope and sent to the computer for analysis with LabVIEW. The output of the oscilloscope is shown in Figure 26. There is one very short pulse, which is less than 10 us, to avoid self-heating of the transistor. Using a very short pulse will keep the drain current constant (I_{ds}). The graph also depicts the drain source voltage (V_{ds}), the gate source voltage (V_{gs}) and the function generator generated signal (V_{sig}) [31].

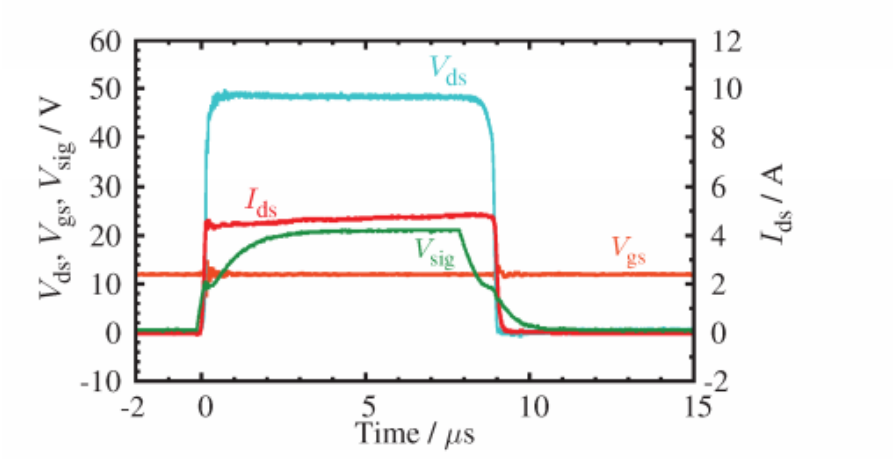

Figure 26 Oscilloscope measured graph from the circuit [31].

By using varying gate source voltages, different I-V graphs can be obtained, as shown in Figure 27. In this figure, an experimental curve tracer is compared with a commercially available curve tracer.

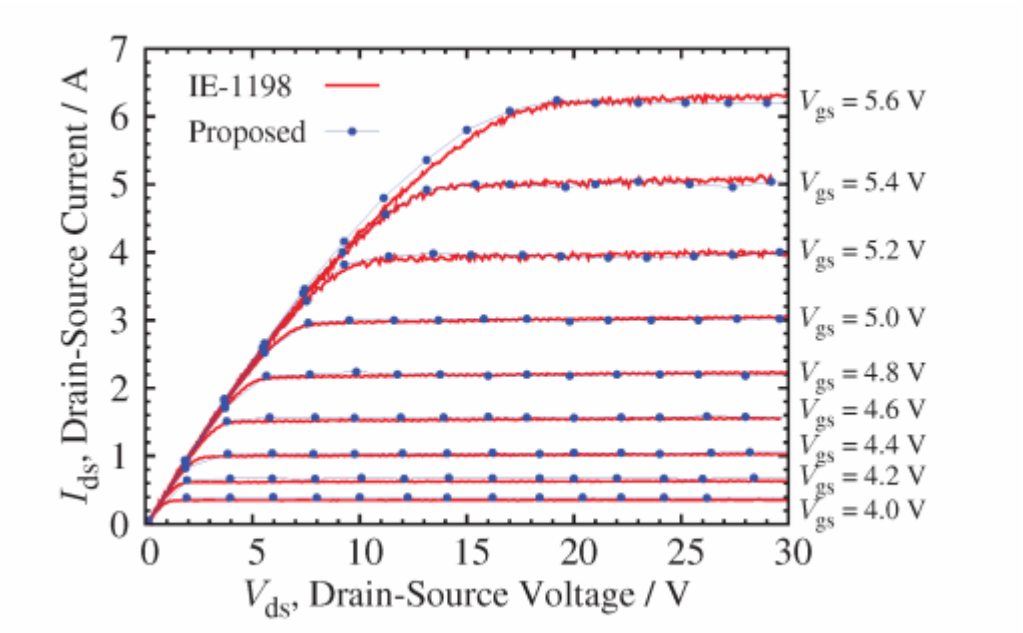

Figure 27 Curve tracer I-V graph [31].

4.2 Testing dynamic current sharing

4.2.1 Double pulse tester

Double pulse testers are used to measure switching performance in a clamped inductive application. The difference from the curve tracer is that switching characteristics rather than static parameters are considered. Double pulse tester comes from the IEC standard

60747-9 annex C “Measuring method for inductive load turn-off current under specified conditions” [28]. The circuit for that kind of application measurement is shown in Figure 28.

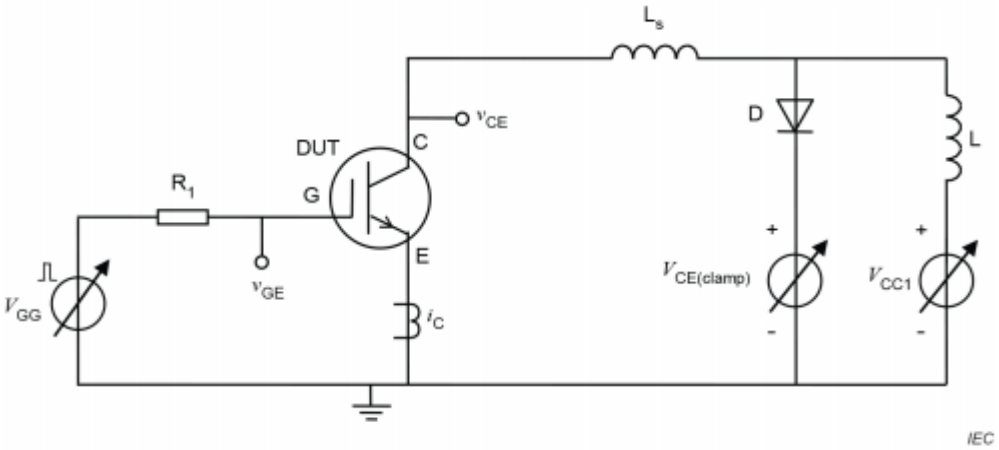

Figure 28 IEC standard for measuring inductive load [28].

DUT is the IGBT in the centre, V_{GG} is the pulse generator, R_1 is the gate resistor, L_s is the unclamped stray inductance, D is the clamping diode, and L is the inductive load. V_{cc1} and $V_{CE(clamp)}$ are the voltage sources. The output of this circuit is shown in Figure 29. The figure illustrates the collector current and the turn-off current rising while the collector emitter voltage is not clamped [28].

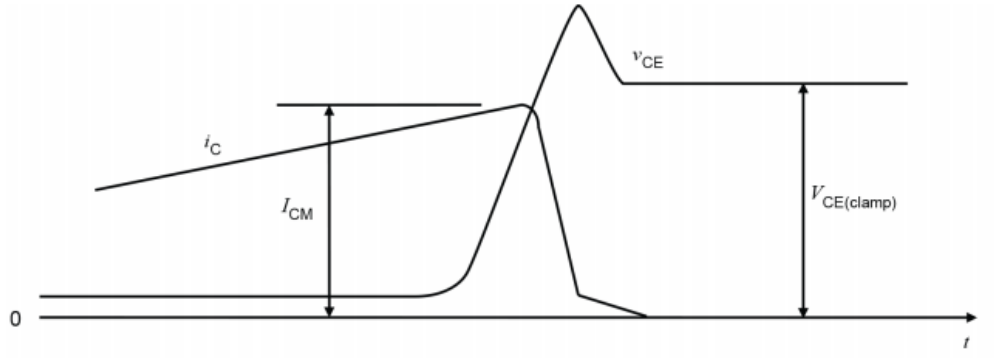

Figure 29 Inductive load current during the IGBT turn-off [28].

According to the IEC standard, for parallel IGBTs, IGBT turn-on and turn-off energy and turn-on and turn-off time are very important parameters, as shown in Figure 31. Delays of the IGBT turn-off will cause high peak collector currents. A circuit for measuring that kind of a parameter is shown in Figure 30. V_{GG1}, V_{GG2} and V_{CC} are voltage sources for the circuit, R_1 and R_2 are gate resistors. D is a freewheeling diode for alternating current from inductance L [28].

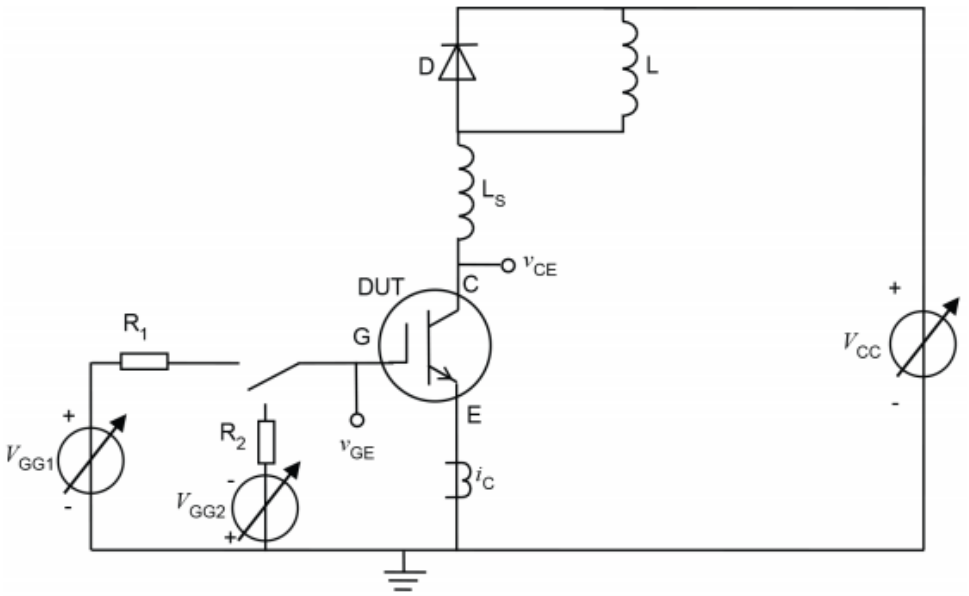

Figure 30 Measurement circuit for IGBT turn-on and turn-off times from the IEC standard [28].

Output of the circuit is shown in Figure 31. The IGBT is turned on and off for two times and the values measured from the second time are observed. Collector current is raised at the first turn-on of the specified level and kept in constant level through the freewheeling diode until the second turn-on. The second pulse shows the following: $t_{d(ON)}$ – turn-on delay time, t_r- rise time, t_{on}- turn-on time, t_i- integral time for calculating turn-on energy, which is calculated by Eq.(5) [32]:

$$E_{ON} = \int_{t1}^{t2} V_{CE}(t) * i_C(t)dt \tag{5}$$

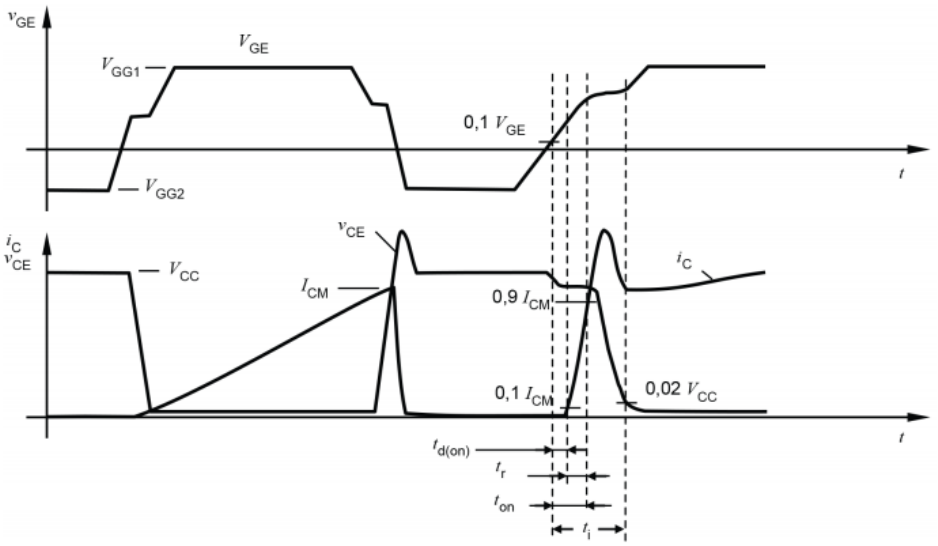

Figure 31 IGBT turn-on energy calculation measurement graph [28].

The same measured values apply both to IGBT turn –on and IGBT turn-off but the measurement is done after the first pulse turn –off, which is shown in Figure 32.

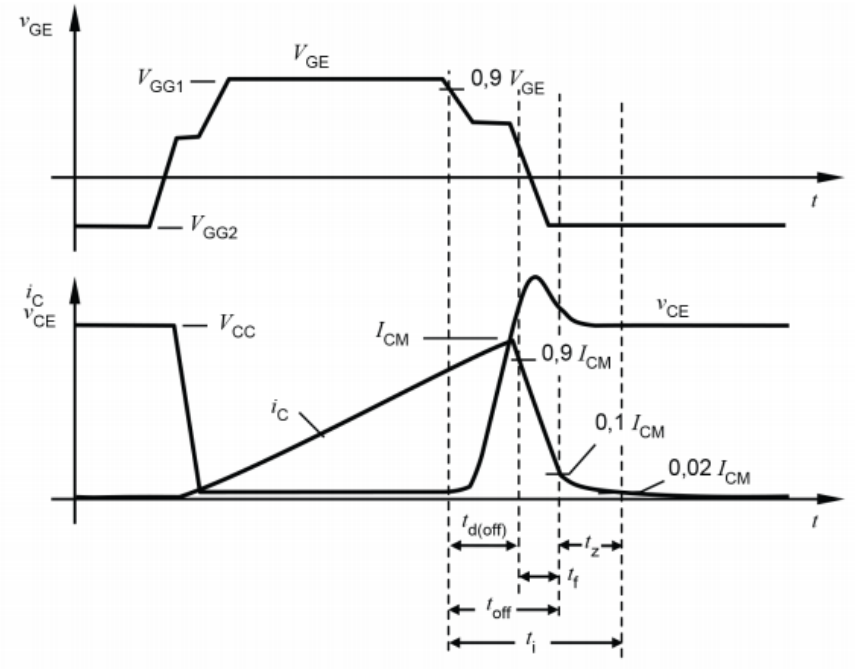

Figure 32 IGBT turn-off energy calculation measurement graph [28].

At the first pulse, $t_{d(OFF)}$ is the turn-off delay time, t_r- the rise time, t_{on}- the turn-on time, t_i- integral time for calculating turn-on energy, which is calculated from Eq.(6) [32]:

$$E_{OFF} = \int_{t3}^{t4} V_{CE}(t) * i_C(t) \tag{6}$$

4.2.2 Parallel pulse tester – 2-pack tester

At the inverter unit manufacture, a parallel pulse tester is used, which simulates inverter unit switching. The term 2-pack tester comes from using the 6-pack mode as the 2-pack mode. So, instead of three half bridges, the inverter unit sees it as the one-half bridge module, as shown in Figure 33.

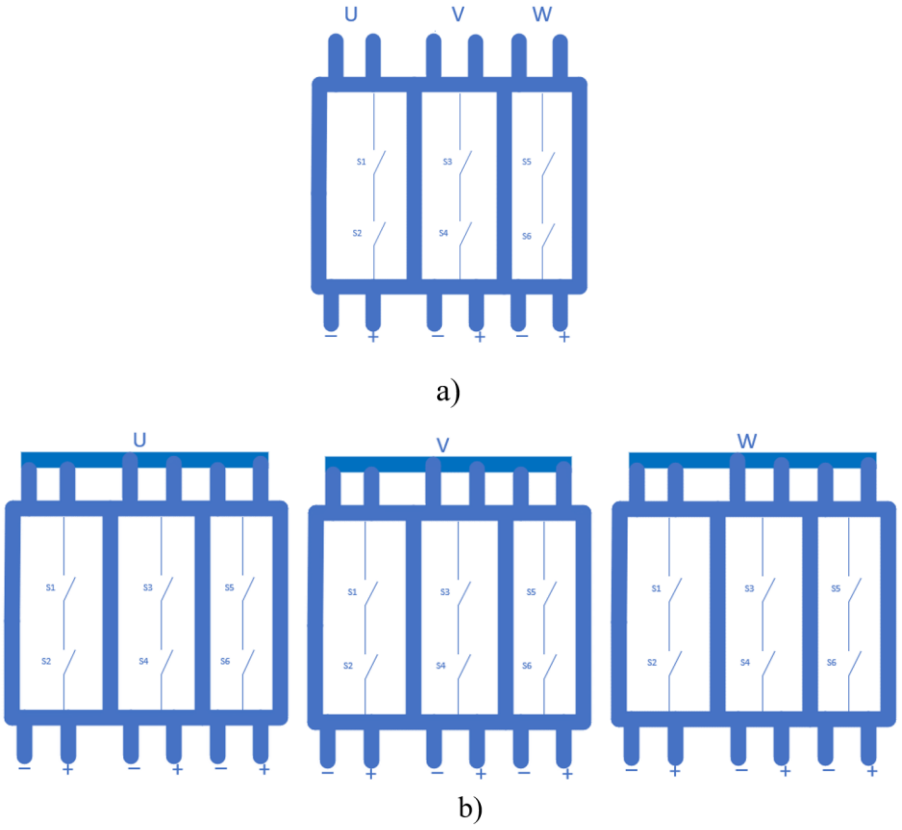

Figure 33 A 3-phase inverter can be realized with a) a single IGBT in 6-pack configuration or b) 2-pack configuration using three 6-packs each in one phase tripling the output current.

The circuit itself is a half inverter unit, which has its own gate driver circuit and power supply. In the input, AC voltage is used, which is alternated with diodes to DC voltage, which loads up the DC capacitors, as shown in Figure 34. From the DC capacitor, current is driven into the IGBT transistor, which has three phase legs that are turned on and off with the same time. For the load, inductive chokes are used. With switches 1 and 2, current path for the upper and lower IGBTs is chosen.

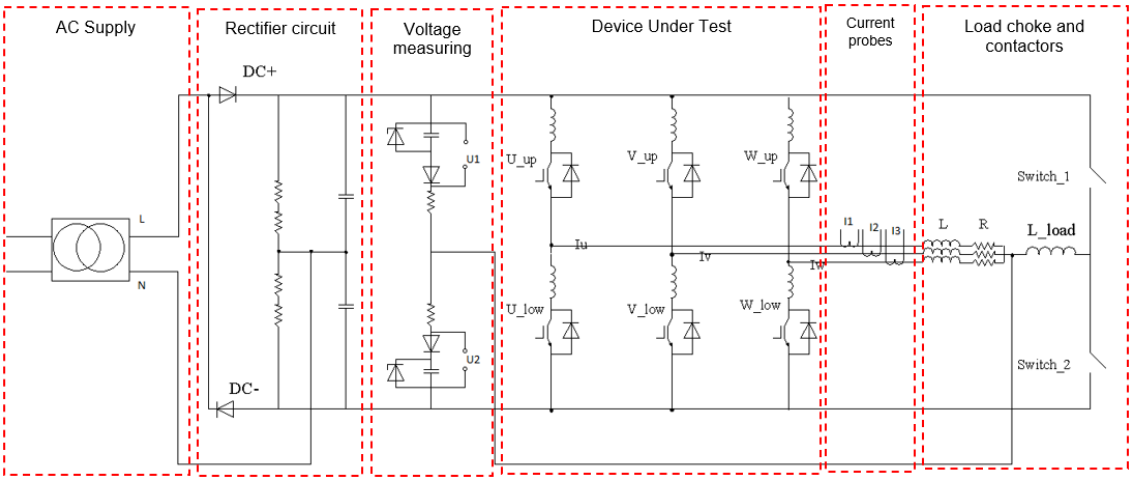

Figure 34 Pulse tester used by inverter unit manufacture.

Through transducers, current is measured and plotted into a graph by an oscilloscope with voltage measurement circuit voltage drop for three branches. The oscilloscope will make comma-separated values (CSV) files where raw data about current values and measured voltage drop can be read out. Raw data graph of the upper IGBT is shown in Figure 35. This test enable testing of IGBT dynamic and static parallel current sharing with one test. At the static current sharing for IGBTs, current is increasing through L/R time constant and current sharing is measured at end of the current increasing step at 850 us. Between 1000 us and 1560 us there is IGBT turn on/off with very short pulse time, one pulse is 25 us. The purpose of this test is to measure IGBT turn on/off delays. After the pulsating phase, current is decreasing through the FWD by L/R constant. Static current sharing for FWD was measured at 1990 us.

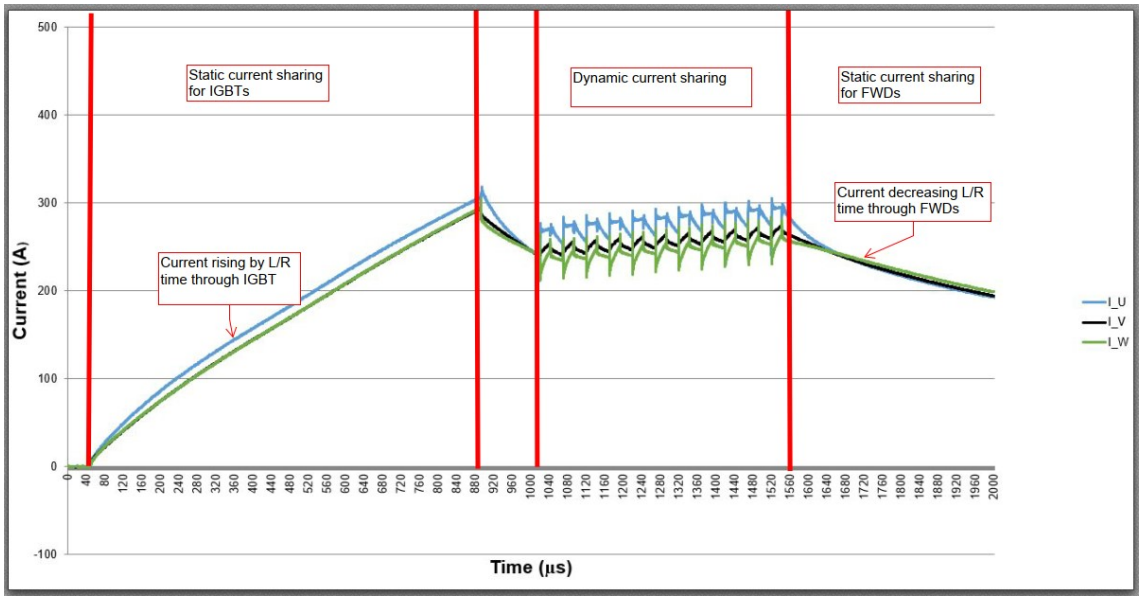

Figure 35 Upper graph of the pulse tester.

4.2.3 Current sharing test limits

Through parallel pulse testers, static and dynamic values are measured against the limits to ensure that IGBT stands for high quality of the inverter unit. For dynamic current measurement, all three phases at the same time during IGBT turn ON/OFF are compared. If there is a big difference in switching delays between IGBTs, then the measured graph will show high peak values, as shown in Figure 36. Fail limit for IGBT is over 100 A peak difference between the branches.

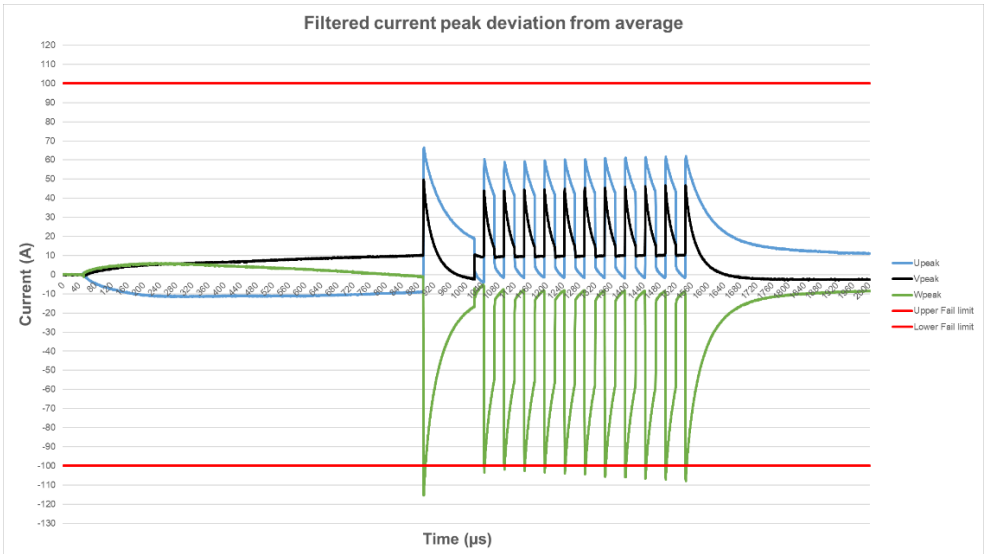

Figure 36 Current peak values at the dynamic state.

For static values, IGBT and FWD current sharing at the steady state current is measured. It will be a test similar to the curve tester but instead of measuring voltage drop current is measured. For IGBTs, the measurement time for current sharing is at 850 us where all three phases are compared to each one. Phase difference for each phase average has percentage described by the FAIL/PASS limit. If one phase difference is more than 8% from all three-phase average currents, then current deviation is too high.

The same calculation method will be applied to FWD current sharing. FWD current sharing is measured at the steady state current at 1990 us. If one phase difference is more than 8% from all three-phase averages, FWD will be failed. Figure 37 below describes graphically the difference of current sharing of one 2% and one 10% IGBT/FWD module.

a)

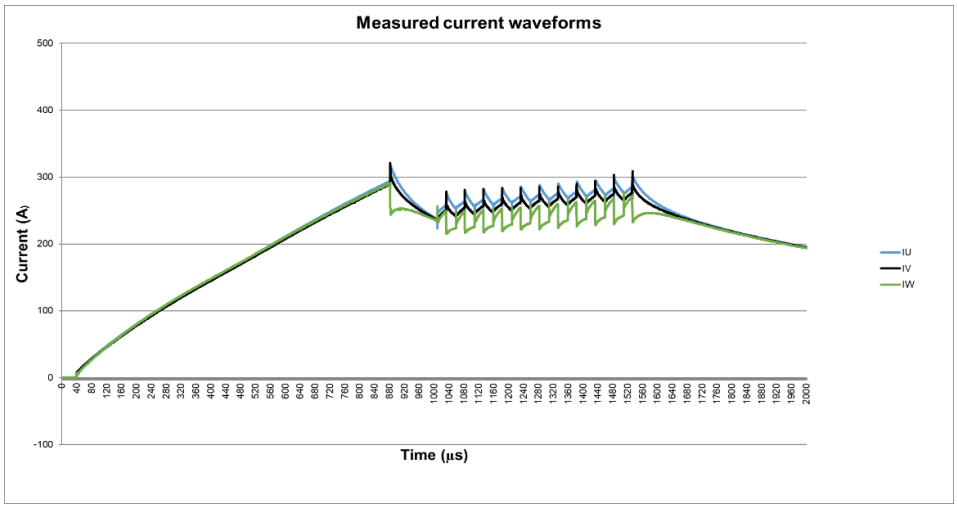

b)

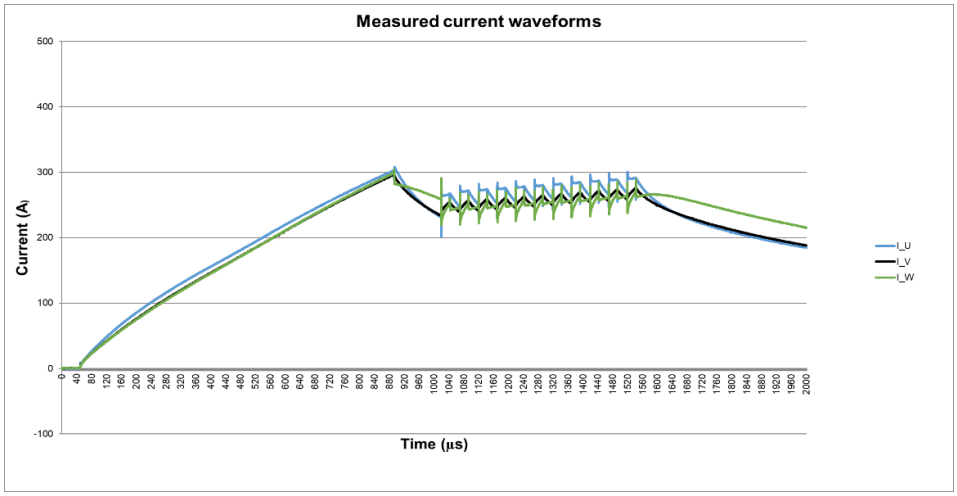

Figure 37 2-pack tested IGBT/FWD module: a) passed – 2% current difference; b) failed - 10% current difference.

In 2020, most of the failures of the 2-pack tester came from FWD static current measurement, as shown in Figure 38, which is also shown in b) Figure 38. It is known that supplier FWD voltage drop at the steady state current will have deviation over 100 mV. For decreasing the IGBT/FWD module failure and scrap rate during 2-pack testing, in the next chapters the feasibility of increasing IGBT/FWD current deviation limit from 8% to 10% will be studied.

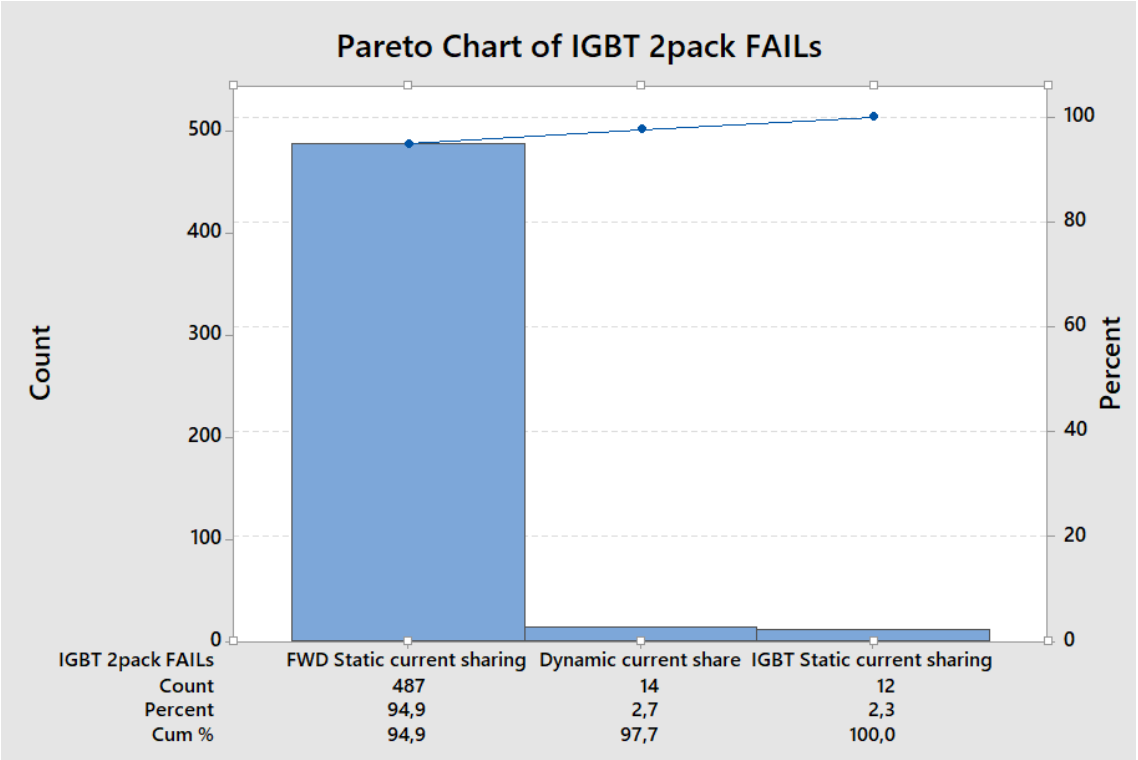

Figure 38 Pareto chart of 2-pack failures.

5 Results & discussion

In subsection 5.1 under the results and discussion chapter, IGBT and FWD characteristics will be measured with a curve tracer. IGBT/FWD modules will be taken after the 2-pack test (Chapter 4.2). The measurement values enable calculation of current sharing between the IGBT module branches. Using the forward voltage, on-state resistance and conduction current, IGBT/FWD power losses can be calculated. The calculated power losses enable estimation of the IGBT/FWD junction temperature. With those values, low and junction temperatures of high current deviation IGBT/FWD modules can be compared. After theoretical analysis, an accelerated life testing with different current deviation IGBT/FWD will be conducted and the results allow for the estimation of the inverter unit lifetime. After comparison and analysis of the lifetime, the decision of raising the current deviation limits can be taken.

5.1 IGBT/FWD power loss estimation

This subsection focuses on the measurement of IGBTs and FWD with a curve tracer and calculation of theoretical current differences between parallel branches. From the current difference, conduction and switching losses for IGBT and FWD can be calculated. After finding the power losses for both chips, I can estimate the theoretical junction temperature. The IGBT/FWD modules chosen were already tested with an 2-pack tester, resulting in 6 pcs of passed – 2% current deviation and 8 pcs of failed – 10% current deviation modules.

5.1.1 Output characteristics measurement

In Figure 39 the schematic of the IGBT module shows an example of six measurement points for IGBT and FWD. There are 12 measurement points for one IGBT module, 6 points for IGBT collector emitter forward voltage and other 6 points for the FWD forward voltage.

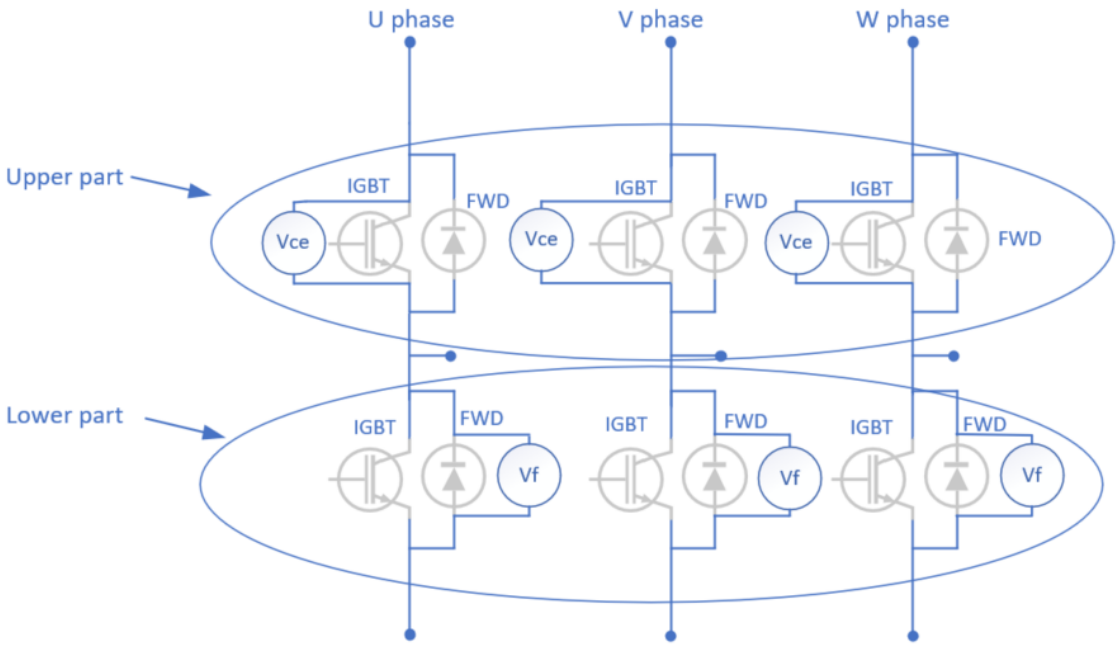

Figure 39 IGBT schematic with measurement points.

Overall amount of the measured IGBT modules was 14 pieces, out of which 6 pieces passed and 8 pieces failed, the list is shown in Appendix 2.

An example of the IGBT collector emitter voltage is shown in Figure 40. The figure points out the maximum and the minimum value of the curve tracer measurement and for comparison, original collector emitter voltage from the supplier datasheet.

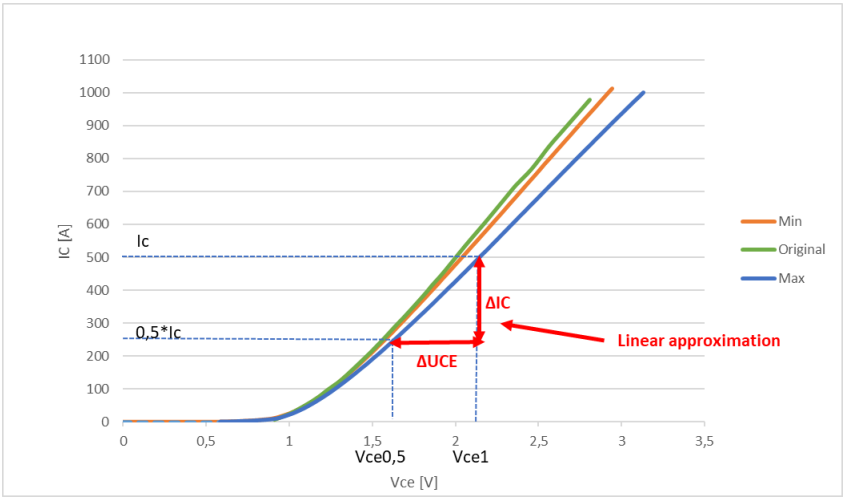

Figure 40 I-V chart for IGBT threshold and on-state resistance calculation

That graph enabled calculation of the IGBT threshold voltage and on-state resistance Eqs.(7) [33] and (8) [33]. Measurements were taken at room temperature.

$$V_{ce0} = 2 * V_{ce05} - V_{ce1}, \tag{7}$$

$$r_{ce0} = \frac{V_{ce1} - V_{ce0.5}}{0.5 * I_c}, \tag{8}$$

where threshold voltage is V_{ce0} and on-state resistance r_{ce0} are both parameters taken from the I-V graph: V_{ce1}, V_{ce05}, I_c , which is shown in Figure 40. Calculated values are presented in Appendix 3. I will use linear approximation because most of the time, the inverter unit operation area is between half I_C to maximum I_C.

Next, focus will be on the FWD threshold and on-state resistance based on Figure 41, which shows the maximum and minimum collector-emitter voltage at on-state and original value from the supplier datasheet. The difference between the minimum and maximum on-states is much wider than for IGBTs.

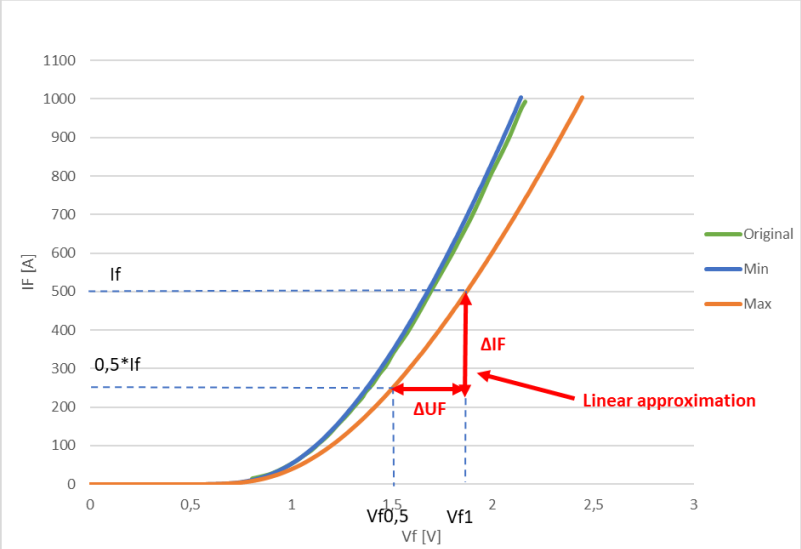

Figure 41 I-V chart for the diode threshold and on-state resistance calculation.

For the FWD, also, threshold voltage and on-state resistance Eqs. (9) [33] and (10) are calculated [33] using the values from the I-V graph.

$$V_{f0} = 2 * V_{f05} - V_{f1}, \tag{9}$$

$$r_{f0} = \frac{V_{f1} - V_{f0.5}}{0.5 * I_f}, \tag{10}$$

where threshold voltage V_{f0} and on-state resistance r_{f0} are both parameters taken from the I-V graph: V_{ce1}, V_{ce05}, I_c , which is shown in Figure 41. Calculated values are presented in Appendix 4. I will use linear approximation because the inverter unit will operate most of the time between half I_f and maximum I_f.

The most complicated part would be to calculate the current difference between parallel branches a) in Figure 42. I need to find i1, i2 and i3 current value for the upper and lower level IGBTs.

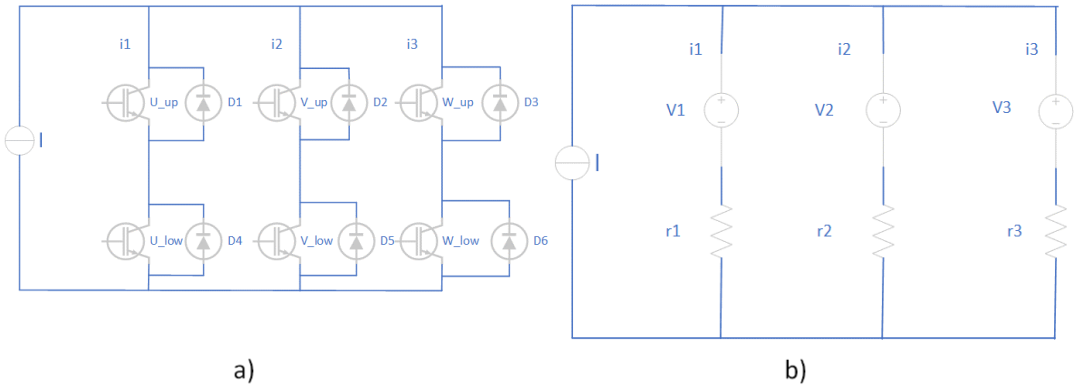

Figure 42 a) Current sharing inside the IGBT module; b) Equivalent circuit from the upper branch.

To find the branch currents, I must find IGBT and FWD equivalent circuit plotted b) in Figure 42. IGBT and FWD saturation voltage will be calculated as the threshold voltage plus on-state resistance times branch collector current Eqs. (1) and (2) in Chapter 3. It is not sufficient to calculate the collector current from the I-V graph and to compare with each other because in the 2-pack mode, IGBT module will have the same potential for all three branches. I will be using Norton´s theorem and transfer IGBT equivalent circuit to Norton circuit. I need to calculate Norton current, voltage, and resistance. Norton voltage is simple to obtain by adding all three branches together in Eq. (11).

$$V_N = v_{ceo(i)} + r_{ce0(i)} * i_i, \tag{11}$$

where V_N is the Norton voltage - potential added to all branches and v_i, r_i, i_i are IGBT threshold voltage, on-state resistance and collector current, which are parameters for each branch. For Norton´s theorem, I can use simple Ohm´s law by finding Norton resistance and current in Eq. (12).

$$V_n = R_N * I_N \tag{12}$$

For finding Norton current, I need to sum up three branches of current sources in Eq. (13).

$$I_N = I + \sum_{n=1}^{n=3} I_{N,n} = I + \sum_{n=1}^{n=3} \frac{v_n}{r_n}, \tag{13}$$

where I_N is Norton current, I - supply current and $\frac{v_n}{r_n}$ is current source. Next, I am calculating Norton resistance by summing up all parallel resistances in Eq. (14).

$$\frac{1}{R_N} = \frac{1}{r_{n(1)}} + \frac{1}{r_{n(2)}} + \frac{1}{r_{n(3)}} \quad (14)$$

Now I will add Norton resistance Eq. (14) and Norton current Eq. (13) inside Ohm's law in Eq. (12), which results in Eq. (15).

$$V_N = \left(\frac{1}{r_{n(1)}} + \frac{1}{r_{n(2)}} + \frac{1}{r_{n(3)}}\right) * \left(I + \sum_{n=1}^{n=3} \frac{v_n}{r_n}\right) \quad (15)$$

I will change Norton voltage with Eq. (11) and the result is the collector current i_i in Eq. (16).

$$i_i = \left[\left(\frac{1}{r_{n(1)}} + \frac{1}{r_{n(2)}} + \frac{1}{r_{n(3)}}\right) * \left(I + \sum_{n=1}^{n=3} \frac{v_n}{r_n}\right) - v_i\right] / r_i \quad (16)$$

The calculated values are presented in Appendix 5.

5.1.2 IGBT and FWD loss calculations

To calculate the estimated IGBT and FWD conduction, the Kolar and Zach equations were used [34].

First, IGBT conduction power losses are calculated in Eq. (17) [34].

$$P_{on\_igbt} = \frac{V_{ce0} * \sqrt{2} I_v}{2} \left[\frac{1}{\pi} + \frac{M}{4} cos\phi\right] + r_{ce0} * I_v^2 \left[\frac{1}{8} + \frac{M}{3\pi} cos\phi\right], \quad (17)$$

where $\sqrt{2} * I_v$ is the calculated losses based on the pulsating current, m - modulation index – (1,15), V_{ce0} is the threshold voltage and r_{ce0} - on-state resistances of the IGBT. Conduction losses are shown in Appendix 6.

In the conduction loss equation, cos ϕ is 0.87 so that the inverter unit is working at the motoring mode, power goes from the network to the load. Current difference from subsection 5.1.1 has been added under I_v, it is summed up for the load current I_{out} , which is 850 A. Conduction losses have been calculated so that the parameters of one branch are multiplied by three. Branch current deviation is also multiplied by three.

Conduction losses are also calculated for FWD in Eq. (18) [34].

$$P_{on\_FWD} = \frac{V_{f0} * \sqrt{2} * I_v}{2} \left[\frac{1}{\pi} + \frac{M}{4} cos\phi\right] + r_{f0} * I_v^2 \left[\frac{1}{8} + \frac{M}{3\pi} cos\phi\right], \quad (18)$$

where $\sqrt{2} * I_v$ is the calculated losses based on the pulsating current, m is the modulation index – (1,15), V_{f0} threshold voltages, r_{f0} on-state resistance for FWD.

All the other parameters are the same as for IGBT conduction loss calculation. Conduction power losses for FWD are presented in Appendix 6.

To get the overall power loss for IGBT and FWD, it is required to calculate also the switching losses. Eq. (19) [35] will be used for calculating the switching losses for IGBT. Switching losses contain the amount of energy for a single IGBT chip to turn on E_{on} and turn off E_{off}. Switching losses are estimated only for an inductive load and there is an error margin for real electric motor application.

$$P_{sw\_igbt} = \frac{E_{isw}}{\pi * V_{ref} * I_{ref}} * U_{dc} * \sqrt{2} * I_v * f_{sw}, \quad (19)$$

where E_{isw} is the sum of turn-on and turn–off energies from IGBT, which will be taken from the supplier datasheet [36]. U_{dc} is DC-link voltage, $\sqrt{2} * I_v$ is calculated losses based on the pulsating current, which would be the same as those used in the conduction loss calculation. Thermal switching frequency f_{sw} would be 2 kHz. Reference voltage V_{ref} and current I_{ref} are used as normalised current and voltage to extract E_{on} and E_{off}. Switching losses for IGBT are presented in Appendix 7.

Switching power losses have been calculated also for FWD, as shown in Eq. (20) [35].

$$P_{sw\_FWD} = \frac{E_{dsw}}{\pi * V_{ref} * I_{ref}} * U_{dc} * \sqrt{2} * I_v * f_{sw}, \quad (20)$$

where E_{dsw} is reverse recovery energy for FWD taken from the supplier datasheet [36]. There is marked also DC-link voltage U_{dc} and $\sqrt{2} * I_v$ is calculated losses based on the pulsating current. Similar to the IGBT switching loss calculation, thermal switching frequency f_{sw} = 2 kHz, V_{ref} and I_{ref} are used as normalised current and voltage to extract E_{on} and E_{off} from the datasheet curves. Switching losses for FWD are presented in Appendix 7.

To obtain the overall power loss for IGBT and FWD, I will sum up the conduction losses and the switching losses. The histogram in Figure 43 shows the passed and failed modules, which were first tested at the 2-pack tester and then analysed by a curve tracer and the power losses were calculated. The calculated values are presented in Appendix 8.

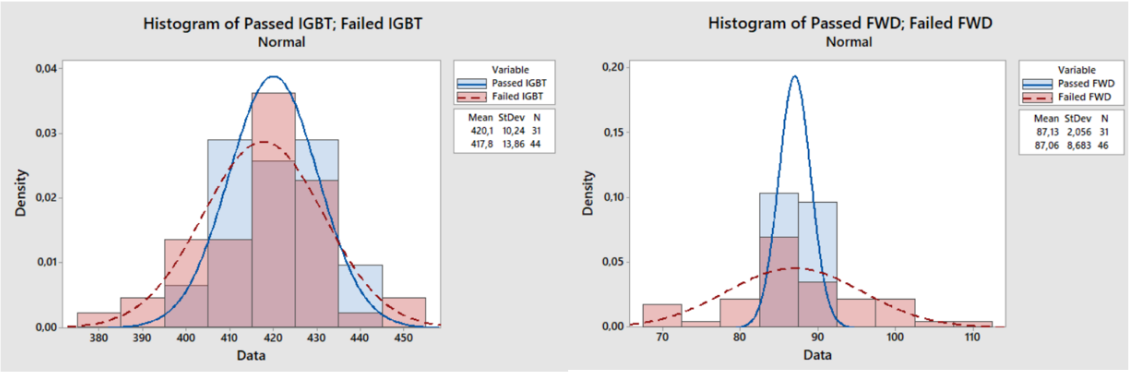

a) b)

Figure 43 Histogram of power losses between failed and passed modules: a) IGBT; b) FWD.

It can be seen from the histogram that the variation between the passed and failed modules for a FWD chip is quite large. Standard deviation for the passed modules is 2.056 and failed modules four times bigger - 8.683. IGBT chips have minor difference in power losses and that is the reason why the 2-pack tester gave no failures for IGBT current difference.

5.1.3 IGBT and FWD junction temperature calculation

In subsection 5.1.2, conduction and switching losses for IGBT and FWD were calculated. Now I can use those results for calculating junction temperature for both devices, as shown in Figure 44 Equivalent circuit of thermal resistance.

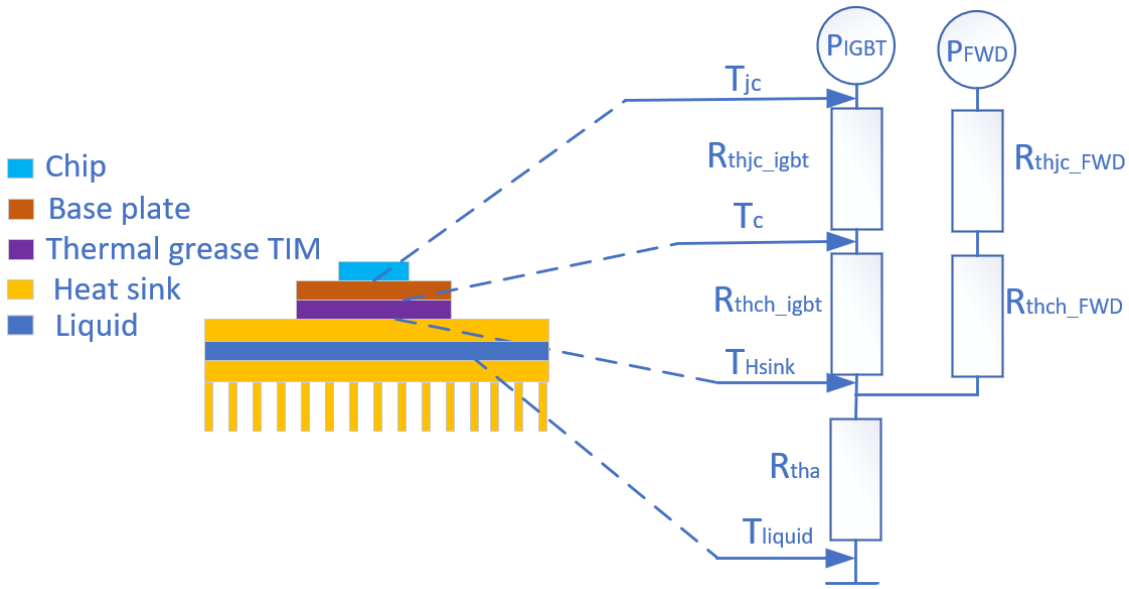

Figure 44 Equivalent circuit of thermal resistance [37].

First, I will sum up the conduction losses and the switching losses in Eq. (21) [24].

$$P_{igbt} = P_{on\_igbt} + P_{sw\_igbt}, \tag{21}$$

where P_{on_igbt} is the IGBT conduction power losses, P_{sw_igbt} is the IGBT switching power losses and P_{igbt} is the IGBT summed power loss.

To obtain the overall IGBT module losses, I need to calculate lead resistance power losses by Eq. (22) [24].

$$P_{lead} = \frac{\left(\frac{I_{out}}{3}\right)^2 * R_{lead}}{2}, \tag{22}$$

where R_{lead} is the IGBT module lead resistance from the terminal to the chip. This particular value was not indicated in the supplier datasheet, but I used the value from similar other 6-pack modules; value $R_{lead} = 0.3\ m\Omega$ [38]. Lead power losses from the terminal to the chip P_{lead} are calculated per switch. After obtaining the lead power losses, I can sum up the overall power loss of the module in Eq. (23) [24]. This equation also describes added FWD power losses, which are required to calculate the whole module power losses.

$$P_{module} = (P_{IGBT} + P_{FWD} + P_{lead}) * 6, \tag{23}$$

where P_{mod} is the IGBT module power losses, including IGBT and FWD chip power losses and losses from lead resistance. It is multiplied by six pieces because there are three upper and lower level parallel chips.

Next, I need the supplier datasheet value for the junction to case resistance R_{thjc_igbt}. By using this value and the power losses of the IGBT, I can calculate the temperature difference between the junction to case by Eq. (24) [24].

$$\Delta T_{jc\_igbt} = P_{IGBT} * R_{thjc\_igbt}, \tag{24}$$

where ΔT_{jc_igbt} is the temperature difference between the IGBT junction and the case. R_{thjc_igbt} is the thermal resistance from the IGBT junction to case taken from the supplier datasheet - $R_{thjc\_igbt} = 0{,}060\ K/W$ [36]. After finding the temperature difference between the junction and the case, I can calculate the temperature between the case and the heatsink by Eq. (25) [24].

$$\Delta T_{ch\_igbt} = P_{IGBT} * R_{thch\_igbt}, \tag{25}$$

where ΔT_{ch_igbt} is the temperature between the IGBT case and heatsink. R_{thch_igbt} is the thermal resistance case to heatsink taken from the supplier datasheet $R_{thch\_igbt} = 0.0167$

K/W [36]. The thermal grease conductivity is included in the R_{thch_igbt}. In the accelerated life testing, I will be using a graphite sheet the thermal conductivity of which is different from grease.

To calculate heatsink temperature, it is required to sum up cooling liquid temperature by the IGBT module power loss multiplied by the heatsink thermal resistance value in Eq. (26) [24].

$$T_{Hsink} = T_{liquid} + P_{module} * R_{tha}, \tag{26}$$

where T_{Hsink} is the heatsink temperature, R_{tha} is the heatsink thermal resistance value supplied to heatsink manufacturer $R_{tha} = 0.0128\, K/W$, scaled to the area of one IGBT module. T_{liquid} is the temperature of the cooling liquid, 55 °C. To calculate the IGBT case temperature, it is required to sum up heatsink temperature with the temperature difference between the case to heatsink in Eq. (27) [24] and to obtain the IGBT junction temperature, I will add the temperature difference between the junction to case in Eq. (28) [24].

$$T_c = T_{Hsink} + \Delta T_{ch\_igbt}, \tag{27}$$

$$T_{jc} = T_{Hsink} + \Delta T_{jc\_igbt} + \Delta T_{ch\_igbt}, \tag{28}$$

where T_c is the IGBT case and the T_{jc} is the junction temperature from the equations above.

After obtaining the IGBT junction temperature, I will calculate the FWD junction temperature. I need to sum up FWD conduction and switching power losses in Eq. (29) [24].

$$P_{FWD} = P_{on\_FWD} + P_{sw\_FWD}, \tag{29}$$

where P_{sw_FWD} is the FWD switching power losses, P_{on_FWD} is the conduction power losses and P_{FWD} is the overall power loss.

Similar to the IGBT chip, it is required to calculate the temperature difference between the junction to case in Eq. (30) [24] and the case to heatsink in Eq. (31) [24].

$$\Delta T_{jc\_FWD} = P_{FWD} * R_{thjc\_FWD}, \tag{30}$$

where ΔT_{jc_FWD} is the temperature difference between the junction to case and R_{thjc_FWD} is the thermal resistance from the FWD junction to case taken from the supplier datasheet $R_{thjc\_FWD} = 0.1\ K/W$ [36].

$$\Delta T_{ch\_FWD} = P_{FWD} * R_{thch\_FWD}, \tag{31}$$

where ΔT_{ch_FWD} is the temperature difference between the case to heatsink and R_{thch_FWD} is the thermal resistance case to heatsink taken from the supplier datasheet $R_{thch\_FWD} =$ 0.0167 K/W [36]. It should be noted that thermal grease was already added into the thermal resistance value. In the accelerated life testing, I will be using graphite sheet, which has thermal conductivity different from that of grease. Using Eq. (26) [24] for obtaining the temperature for heatsink, I can calculate the FWD case temperature in Eq. (32) [24] and the junction temperature in Eq. (33) [24].

$$T_{c\_FWD} = T_{Hsink} + \Delta T_{ch\_FWD} \tag{32}$$

$$T_{jc\_FWD} = T_{Hsink} + \Delta T_{jc\_FWD} + \Delta T_{ch\_FWD}, \tag{33}$$

where T_c is the case and T_{jc} is the junction temperature.

Results shown in Figure 45 are plotted as a boxplot of temperature variation between the passed and failed modules. List of all temperatures is available in Appendices 9 and 10.

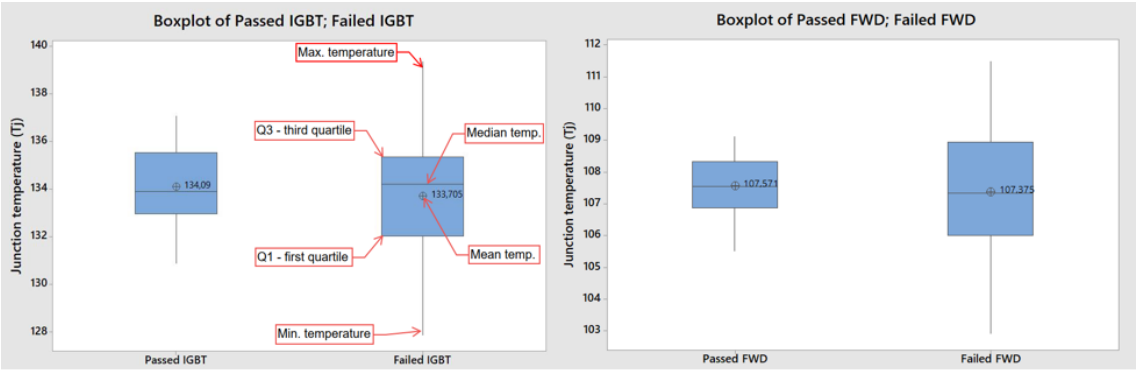

Figure 45 Boxplot of temperature variation: a) IGBT; b) FWD.

In the boxplot, there are five results to be read: maximum, minimum, median, first quartile and third quartile. Maximum temperature is the highest temperature in the variation and minimum indicates the lowest temperature. Median is the value where 50% are higher values and another 50% are lower than median. First quartile indicates the position where 25% of the values are lower than first quartile and 75% are higher. Third quartile means

that 75% of the values are lower than the third quartile and 25% of the values are higher. I am using this boxplot to show the difference between the maximum and minimum temperatures. Figure 45 a) shows the temperature variation between the passed and failed IGBT modules chips. Maximum and minimum temperatures are much higher for failed modules than passed modules and maximum temperature difference is 11 °C and 6 °C for passed modules. Quartile 1 and quartile 3 and median play a minor role here because the temperature difference there is maximum three degrees.

FWD junction temperature variation is quite the same as shown in Figure 45 b). Maximum and minimum temperature difference for failed modules is almost 9 °C and 4 °C for passed modules. Comparison of quartile 3 for passed and failed modules shows that failed modules have a much wider variation. Subsection 5.2 will show the value of the gap between the minimum and maximum junction temperatures that will have effect on the IGBT/FWD module lifetime.

5.2 Accelerated life test

In this subsection, IGBT/FWD modules will be used in accelerated life testing (ALT) for estimating their lifetime in real applications. In the previous subsection, I was calculating IGBT/FWD branch temperature for different passed and failed modules. Now I will take three failed and passed IGBT/FWD modules and put them inside inverter units to see what the actual temperatures will be. It should be noted that I will not use exactly the same serial number IGBT/FWD modules that were compared in subsection 5.1.

5.2.1 Accelerated life test setup

In the tester setup, there are two inverter units connected in parallel through a common DC-link, as shown in Figure 46. One inverter unit contains three IGBT/FWD 6-pack modules that work in 2-pack mode. Inverter units are supplied by a three-phase thyristor supply unit. Inverter unit specification is shown in Table 1.

Inverter unit	Input voltage (VDC)	Cos ϕ	Output voltage (AC)	Output frequency (Hz)	Output Current (A)
LC1	*932*	0,87	690	50	850
LC2	932	0,87	690	50	850

Table 1 Inverter units used in ALT test.

Both inverter units are loaded with four pairs of electric motors with overall 800 kW load power. Two 400 kW motors work in parallel on one shaft and the overall power is 800 kW.

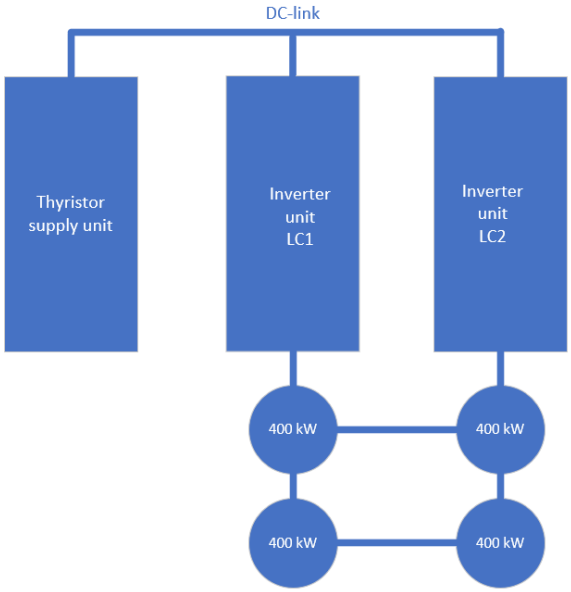

Figure 46 ALT tester setup.

One electric motor specification is shown in Table 2.

Voltage	690	V
Current	395	A
Frequency	50	Hz
Speed	1489	rpm
Power	400	kW
cos φ	0.87	

Table 2 Motor nominal values.

Inverter units are working in different modes. When one inverter unit is operating at the motoring mode, then the other inverter unit is operating in the generation mode. Distribution of losses between IGBTs and diodes depends on the power sign. To get an even amount of power drawn, direction of the power flow is always changed after two periods. Load cycle profile is shown in Figure 47. In section one, the first inverter unit accelerates the motor with constant torque, in section two, the second inverter is ramped up with reference torque. Both inverter units are running in the same direction, but they have opposite torque in section three. In section four, the first inverter unit is decelerating to zero speed while the second inverter unit has zero torque reference. In section five, inverter units are cooled down to ambient temperature.

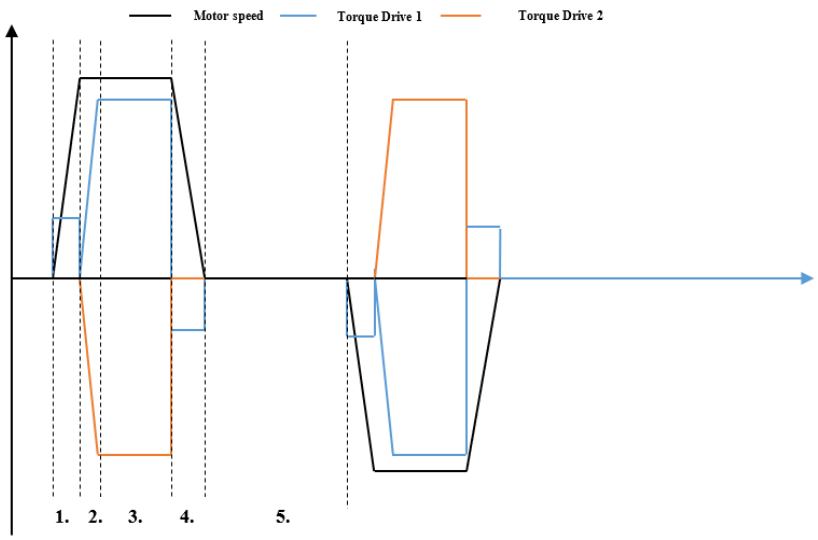

Figure 47 ALT cycle profile.

Figure 48 shows the load cycle and measured temperatures from the ALT testing. The load cycle is 180 s long, which consists of 60 s power cycling and 60 s of cool down period. On the graph, LC1 Tc is the IGBT module case temperature and LC1 Tj is the virtual junction temperature calculated by the inverter unit. LC1 and LC2 are inverter units where in LC1, IGBT modules that have good results from the 2-pack tester and in LC2, failed modules are shown. There is no difference in terms of case and junction temperatures between the inverter units; however, those values are calculated for the whole IGBT module and no single chip temperature is shown.

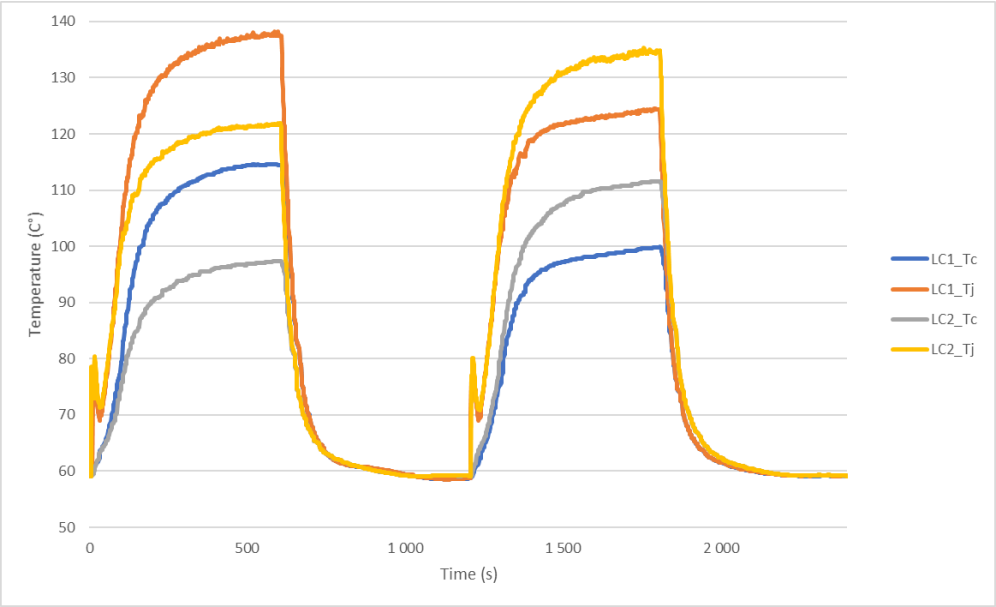

Figure 48 ALT cycle time and temperatures for inverter units: LC1, LC2.

5.2.2 Passed and failed IGBT and FWD lifetime

Passed and failed modules have been taken after the 2-pack test result and assembled into the inverter unit LC1 and LC2, as shown in Table 1. Inside the passed and failed module power plate there are drilled holes in the J-type thermocouples. Thermocouples locations are shown in the IGBT module drawing in Figure 49. There are together 6 pcs thermocouples inside one IGBT/FWD module. Three thermocouples are put under lower level IGBT and upper level FWD chips. Thermocouples locations and names are shown in Appendix 11.

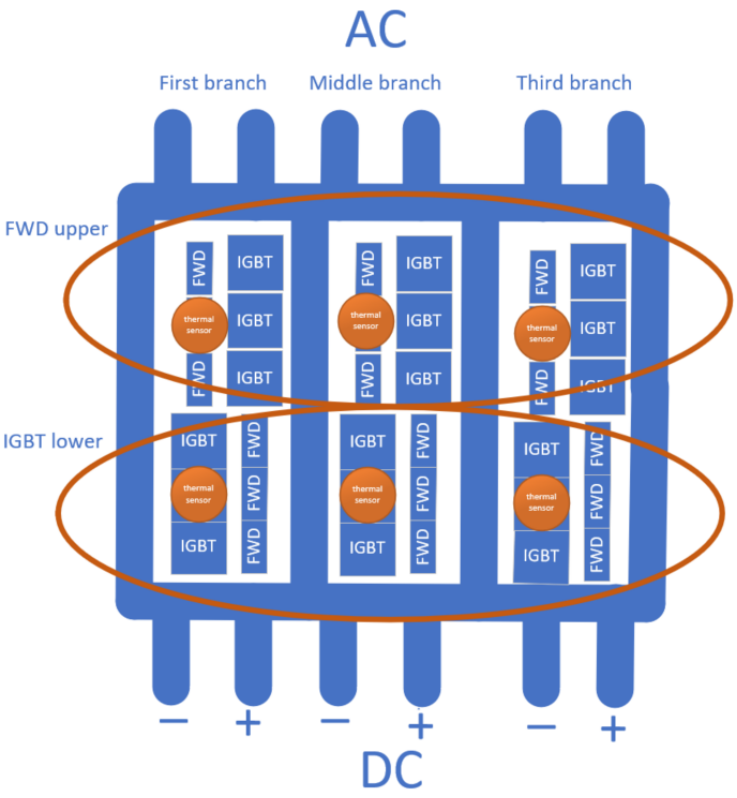

Figure 49 J-type thermocouples locations.

Results from the testing are shown in Figures 50 and 51 where values from ALT testing are plotted. It is clearly demonstrated that in the LC1 inverter unit where passed IGBT modules are installed, the chip values have more equal temperature difference share compared to the inverter unit LC2 where failed IGBT modules are installed in Figure 50. However, failed IGBT modules chips reveal that there is almost 20 °C cap between three baseplate temperatures and other baseplate values.

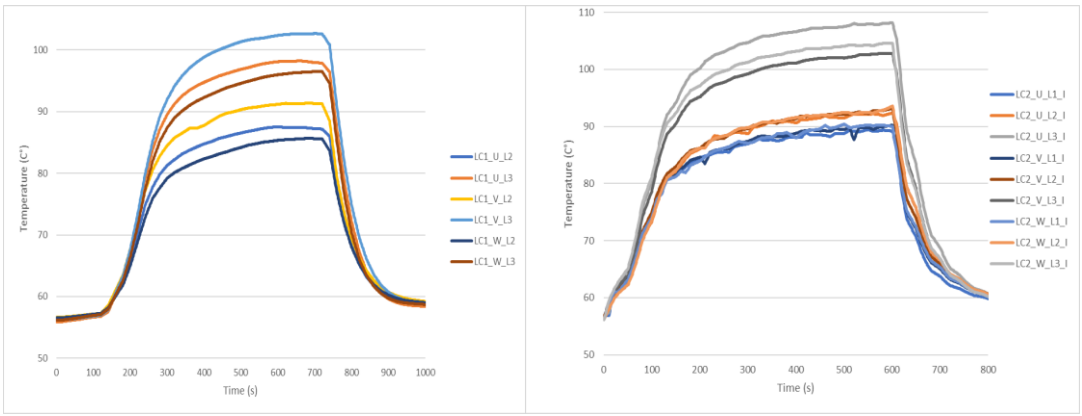

Figure 50 IGBT baseplate temperatures: a) LC1 b) LC2.

The same can be seen in Figure 51 where FWD values are plotted. LC1 baseplate temperatures have much equal share than LC2 module baseplate temperatures. It should be noted that LC1 has 3 J-type thermocouples installed and LC2 has 6 J-type thermocouples; therefore, there is less data in the graph for LC1. J-type thermocouple measurements are presented in Appendix 12.

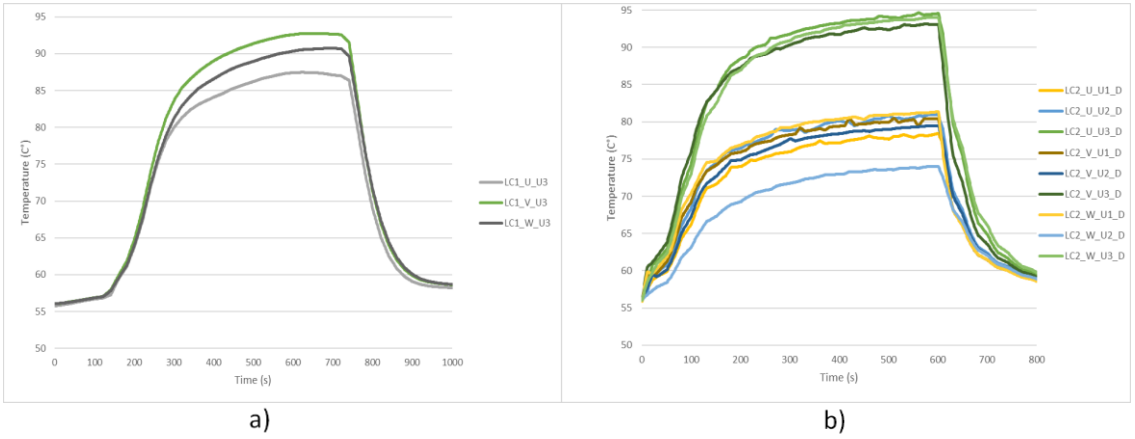

Figure 51 FWD baseplate temperatures: a) LC1 b) LC2.

It should be noted that statistically there is not enough thermocouples measurement points for comparing those results with theoretical ones because there is a possibility to test only two inverter units at the time; therefore, I have only six IGBT/FWD modules. Also, junction temperatures were calculated in subsection 5.1.3 but they cannot be directly compared to thermocouples results. However, theoretical results showed that there is higher variation in failed modules and the same is with baseplate temperatures.

Figure 52 shows the calculated lifetime from the measured thermocouples values, which are presented in Appendix 12. Temperature values of the LC1 and LC2 inverter units

passed and failed IGBT/FWD modules are plotted there. Resulting from subsection 4.2.3, it should be reminded that passed modules have current difference around 2% and failed modules around 10%. Both inverter units have quite large variation for IGBT and FWD lifetime. For passed modules, the highest lifetime would be 940 k cycles for W phase branch 2 lower IGBT chip and the lowest cycling time 127 k cycles for V phase branch 3 lower IGBT chip. Failed modules maximum cycles would be W phase branch 2 upper FWD with 6940 k cycles and for the lowest cycling time would be U phase branch 3 lower IGBT chip with 76 k cycles.

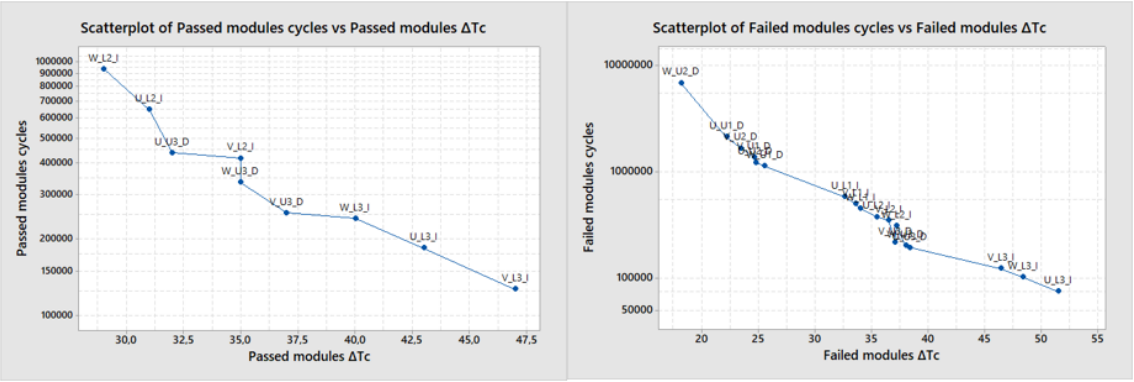

a) b)

Figure 52 Module cycles vs. temperature rise: a) passed IGBT/FWD branches, b) failed IGBT/FWD branches.

For failed modules, the lowest lifetime was not in FWD but in IGBTs, because in the inverter mode, IGBTs have higher temperatures than in for alternating mode where FWD will get most of the load. It was indicated in subsection 5.1.3 that FWD has wider variation than IGBTs but in the real application, it is playing a minor role. For comparing tested modules temperature with 2-pack tester results, the highest temperatures should be found in the branches other than the thermocouples measurement gives. There might be several factors involved, but one explanation might be the graphite sheet that has more equal heat flow than thermal grease between heatsink and IGBT baseplate [16].

The calculated operation hours in Table 3 reveal that 2-pack tester limit cannot be raised to 10% because the inverter unit operation hours decrease double times. Those operation hours are calculated just for the current ALT tester setup in subsection 5.2.1.

Inverter unit	IGBT/FWD	Cycles (k)	Working hours (h)
LC1	V phase lower IGBT	127	4233,3
LC2	U phase lower IGBT	76	2533,3

Table 3 Theoretical operation hours of LC1 and LC2 inverter unit.

Operation hours in the field site would be much longer and it depends also on the application where this inverter unit is used. However, the final decision cannot be taken until the operation ending of the inverter unit lifetime. Unfortunately, accelerated life testing takes longer time than this thesis timeframe and the conclusions for this thesis are based on the theoretical lifetime calculation model.

6 Summary

Focus in this work was on static current sharing for IGBT and FWD chips and on the possibility to raise current sharing testing limits for a 2-pack tester. Altogether 14 pieces IGBT/FWD modules were previously tested with a current sharing tester. From the current sharing tester, 8 IGBT/FWD modules failed the test and their current difference was more than 10% and 6 IGBT/FWD modules passed the test and their current difference was below 2%. The purpose of this thesis was to analyse and determinate if it is possible to raise the testing limit from 8% to 10%, which means that failed modules can be used in production inverter units. My analyses included characteristic analysis with a curve tester for those IGBT/FWD modules. From the curve tracer I-V graphs, threshold voltage, on-state resistance and collector/diode current were calculated. Those values enabled calculation of IGBT and FWD conduction and switching losses. As a result, I calculated the theoretical junction temperature for IGBTs and FWD. The results showed that failed IGBT/FWD modules have much wider junction temperature difference than passed modules. If the junction temperature has large variation between IGBG/FWD module branches, it causes the risk that some of the IGBT/FWD chips will wear out sooner than others and can decrease inverter unit lifetime. To further analyse the testing limits, accelerated life testing was conducted with passed and failed IGBT/FWD modules. In the accelerated life testing, I used two inverter units both of which had 3 passed 2-pack modules and 3 failed 2-pack modules. For both modules, thermocouples were installed to measure baseplate temperature under each branch. Baseplate temperatures were taken after running the inverter units for a few days at full load. Results showed that passed modules had more equal temperature share between the branches. However, in 3 branches, failed modules had 20 °C higher temperature than other branches. Accelerated life testing will usually take several months up to half a year and for that reason, I was using a theoretical model by applying baseplate temperature and operation cycle to calculate maximum operation working hours to those modules. Results showed that the lowest calculated operation hours were 3 branches in the failed IGBT/FWD modules. Comparing the results with the passed modules, the operation time was two times longer than that of failed ones. Inverter unit lifetime depends on the IGBT/FWD module, which has least operation hours and with failed modules, it would have two times shorter lifetime than with passed modules. For that reason, 2-pack tester limits cannot be risen to 10%

because possible lifetime of the IGBT module will decrease twice as much as for 2% IGBT/FWD module. However, the final decision will be taken after end of the accelerated testing, which is out of this thesis timeframe.

References

[1] Fuji Electric “2MBI1400VXB-170E-54”, https://www.fujielectric.com/products/semiconductor/” 2MBI1400VXB-170E-54.

[2] A.Volke, M.Hornkamp “IGBT modules. Technologies, driver and application” Infineon Technologies AG, Munich, 2017.

[3] T. Saito, Y. Nishimura, F. Momose, A. Hirao, A. Morozumi, Y. Tamai, E. Mochizuki, Y. Takahashi “High reliability packaging technologies for 175deg.C continuous operation in IGBT module” International Conference on Electronics Packaging and iMAPS All Asia Conference , Kyoto, Japan, 2015.

[4] M. Rahimo “Future trends in high-power bipolar metal-oxide semiconductor controlled power semi-conductors” IET Circuits, Devices and Systems 2013.

[5] P. M. Shenoy, S. Shekhawat, Bob Brockway “Application specific 1200V planar and trench IGBTs” Applied power electronics conference and exposition, Dallas, USA, 2006.

[6] B. Jayant Baliga “The IGBT device” William Andrew March 2015.

[7] Mitsubishi “NX CM600DXP-34T”, https://www.mitsubishichips.eu/wp-content/uploads/2019/10/Bodos-Power-Systems_15-08_Mitsubishi-Electric-Semiconductor.pdf

[8] Mitsubishi Electric “PM75CG1B120”, https://www.mitsubishielectric.com/semiconductors/products/powermod/intelligentpmod/.

[9] Runau semiconductor, https://www.chinarunau.com/2020-high-quality-disc-type-fully-crimped-high-power-igbt-press-pack-igbt-runau-electronics-3-product/.

[10] Infineon “IKP20N60H3”, https://www.infineon.com/cms/en/product/power/igbt/igbt-discretes/ikp20n60h3/ Infineon IKP20N60H3.

[11] A.S.Bahman, F.Iannuzzo, C.Uhrenfeldt, .Blaabjerg, S.Munk-Nielsen “Modeling of Short-Circuit-Related Thermal Stress in Aged IGBT Modules” IEEE Transactions on Industry Applications, 2017.

[12] M.Held, P. Jacob, G. Nicoletti, P. Scacco, M.-H. Poech “Fast Power Cycling Test for IGBT Modules in Traction Application” Zürich, Switzerland 1997.

[13] AN2019-05 “PC and TC Diagrams” Infineon Technologies AG Munich, Germany, 2019.

[14] Semikron “Skim 63/93 product range”, https://www.semikron.com/products/product-lines/skim/skim-6393.html.

[15] P. Drexhage “Thermal paste application” Semikron application note AN 18-001.

[16] Panasonic “PGS graphite sheet”, https://industrial.panasonic.com/ww/pgs2/soft-pgs.

[17] H. Wang, J. Przybilla, H. Zhang, J. Schiele “The new high reliable press pack IGBT for modular multilever converter in VSC-HVDC applications.” 4th International Conference on HVDC, Xi'an, China, 2020.

[18] F. Wakeman, D. Hemmings, W. Findlay and G. Lockwood, "Pressure contact IGBT testing for reliability" in PCIM Nuremberg, Germany, 2000.

[19] H. Chen, W. Cao, P. Bordignon, R Yi, H. Zhang, W. Shi “Design and testing of the World's first single-level press-pack IGBT based submodule for MMC VSC HVDC applications” IEEE Energy Conversion Congress and Exposition Monteral, Canada 2015.

[20] A. S. Bahman, F.Iannuzzo, C.Uhrenfeldt, .Blaabjerg, S.Munk-Nielsen “Modeling of Short-Circuit-Related Thermal Stress in Aged IGBT Modules” IEEE Transactions on Industry Applications, 2017.

[21] G. J. Riedel, M. Valov “Simultaneous Testing of Wirebond and Solder Fatigue in IGBT Modules” 8th International Conference on Integrated Power Electronics Systems Nuremberg, Germany, 2014.

[22] Y. Bao, Q. Jiang “Summary of Life Prediction and Failure Analysis of IGBT Modules Based on Accelerated Aging Test” 22nd International Conference on Electrical Machines and Systems, Harbin, China, 2019.

[23] R. Schnell “Paralleling of IGBT modules” ABB Switzerland Ltd. Semiconductors, Lenzburg 2013.

[24] B. Backlund, R. Schnell, U. Schlapbach, R. Fischer, E. Tsyplakov “Applying IGBTs” ABB application note 5SYA2053.

[25] Fuji Electric “2MBI300HJ-120-50”, https://www.fujielectric.com/products/semiconductor/.

[26] A.Baschnagel, D. Prindle, S. Geissmann, F. Fischer, S. Hartmann, R, Schnell, G. Pâques, A. Kopta “Paralleling of LinPak power modules” Nuremberg, Germany 2017.

[27] A. Liu, N. Pluschke “Paralleling of medium-power IGBT modules in windmill converter to reduce size and cost” PCIM Asia, June 2019, Shanghai, China.

[28] IEC 60747-9 “Part 9: Discrete devices – Insulated-gate bipolar transistors (IGBTs)” Geneva, Switzerland, 2019.

[29] IEC 60747-2 “Part 2: Discrete devices – Rectifier diodes” Geneva, Switzerland, 2016.

[30] Keysight “Power analyzer/curve tracers”, https://www.keysight.com/zz/en/assets/7018-04763/technical-overviews/5992-0562.pdf.

[31] Y. Nakamuta, M. Shintani, T. Sato, T. Hikihara “A High Power Curve Tracer for Characterizing Full Operational Range of SiC Power Transistors” Yokohama, Japan, 2016.

[32] U. Nicolai “Determining switching losses of Semikron IGBT modules” Nuremberg, Germany, 2014.

[33] D. Graovac, M. Pürschel “IGBT power losses calculation using the data-sheet parameters”, Neubiberg, Germany 2009.

[34] J.W. Kolar, H.Ertl, F. C. Zachv “Calculation of the passive and active component stress of three phase PWM converter systems with high pulse rate.” Vienna, Austria 1989.

[35] B. Wang, Y. Tang “Calculation of power consumption and junction temperature of IGBT module in inverter” International Conference on Energy Engineering, 2021, Shenzhen, China.

[36] Fuji “6MBI450V-170-50”, https://www.fujielectric.com/products/semiconductor/model/igbt/6pack.html

[37] N. Kerstin, M. Schulz “The challenge of accurately analyzing thermal resistances” PCIM Europe, Nuremberg, Germany, 2014.

[38] Semikron “SKiM429DG17E44F”, https://www.semikron.com/products/product-lines/skim/skim-6393.html.

Appendix 1 – Non-exclusive licence for reproduction and publication of a graduation thesis[1]

I Tõnis Talviste

1. Grant Tallinn University of Technology free licence (non-exclusive licence) for my thesis “Determination and Analysis of IGBT Module Current Sharing Testing Limits”, supervised by Indrek Roasto.
   1.1. to be reproduced for the purposes of preservation and electronic publication of the graduation thesis, incl. to be entered in the digital collection of the Library of Tallinn University of Technology until expiry of the term of copyright;
   1.2. to be published via the web of Tallinn University of Technology, incl. to be entered in the digital collection of the Library of Tallinn University of Technology until expiry of the term of copyright.
2. I am aware that the author also retains the rights specified in clause 1 of the non-exclusive licence.
3. I confirm that granting the non-exclusive licence does not infringe other persons' intellectual property rights, the rights arising from the Personal Data Protection Act or rights arising from other legislation.

09.05.2021

1 The non-exclusive licence is not valid during the validity of access restriction indicated in the student's application for restriction on access to the graduation thesis that has been signed by the school's dean, except in case of the university's right to reproduce the thesis for preservation purposes only. If a graduation thesis is based on the joint creative activity of two or more persons and the co-author(s) has/have not granted, by the set deadline, the student defending his/her graduation thesis consent to reproduce and publish the graduation thesis in compliance with clauses 1.1 and 1.2 of the non-exclusive licence, the non-exclusive license shall not be valid for the period.

Appendix 2 – IGBT/FWD curve tracer measurement list

Passed - around 2% current difference				
Serial number 1	**Serial number 2**	**Serial number 3**	**Serial number 4**	**Description**
U_UL	U_UL	U_UL	U_UL	U phase Upper lever IGBT/FWD
U_LL	U_LL	U_LL	U_LL	U phase Lower lever IGBT/FWD
V_UL	V_UL	V_UL	V_UL	V phase Upper lever IGBT/FWD
V_LL	V_LL	V_LL	V_LL	V phase Lower lever IGBT/FWD
W_UL	W_UL	W_UL	W_UL	W phase Upper lever IGBT/FWD
W_LL	W_LL	W_LL	W_LL	W phase Lower lever IGBT/FWD
Serial number 5	**Serial number 6**			**Description**
U_UL	U_UL			U phase Upper lever IGBT/FWD
U_LL	U_LL			U phase Lower lever IGBT/FWD
V_UL	V_UL			V phase Upper lever IGBT/FWD
V_LL	V_LL			V phase Lower lever IGBT/FWD
W_UL	W_UL			W phase Upper lever IGBT/FWD
W_LL	W_LL			W phase Lower lever IGBT/FWD

Failed - around 10% current difference				
Serial number 1	**Serial number 2**	**Serial number 3**	**Serial number 4**	**Description**
U_UL	U_UL	U_UL	U_UL	U phase Upper lever IGBT/FWD
U_LL	U_LL	U_LL	U_LL	U phase Lower lever IGBT/FWD
V_UL	V_UL	V_UL	V_UL	V phase Upper lever IGBT/FWD
V_LL	V_LL	V_LL	V_LL	V phase Lower lever IGBT/FWD
W_UL	W_UL	W_UL	W_UL	W phase Upper lever IGBT/FWD
W_LL	W_LL	W_LL	W_LL	W phase Lower lever IGBT/FWD
Serial number 5	**Serial number 6**	**Serial number 7**	**Serial number 8**	**Description**
U_UL	U_UL	U_UL	U_UL	U phase Upper lever IGBT/FWD
U_LL	U_LL	U_LL	U_LL	U phase Lower lever IGBT/FWD
V_UL	V_UL	V_UL	V_UL	V phase Upper lever IGBT/FWD
V_LL	V_LL	V_LL	V_LL	V phase Lower lever IGBT/FWD
W_UL	W_UL	W_UL	W_UL	W phase Upper lever IGBT/FWD
W_LL	W_LL	W_LL	W_LL	W phase Lower lever IGBT/FWD

Appendix 3 – IGBT V_{ce0} and R_{ce0} measurements

Passed module				Failed module			
Branch	**Serial number**	**IGBT Vce0 [V]**	**IGBT Rce0 [mΩ]**	**Branch**	**Serial number**	**IGBT Vce0 [V]**	**IGBT Rce0 [mΩ]**
U_UL	Serial number 1	1,1029	2,0373	U_UL	Serial number 1	1,1197	1,9112
V_UL	Serial number 1	1,0889	2,0417	V_UL	Serial number 1	1,1576	1,8911
W_UL	Serial number 1	1,1119	1,9897	W_UL	Serial number 1	Missing	Missing
U_LL	Serial number 1	1,1233	2,4679	U_LL	Serial number 1	1,1260	2,3921
V_LL	Serial number 1	1,088	2,5179	V_LL	Serial number 1	1,1203	2,3917
W_LL	Serial number 1	1,1277	2,5008	W_LL	Serial number 1	Missing	Missing
U_UL	Serial number 2	1,119	2,0176	U_UL	Serial number 2	1,1399	1,9268
V_UL	Serial number 2	Missing	Missing	V_UL	Serial number 2	1,1356	1,9035
W_UL	Serial number 2	Missing	Missing	W_UL	Serial number 2	1,1362	1,9253
U_LL	Serial number 2	1,1285	2,4194	U_LL	Serial number 2	Missing	Missing
V_LL	Serial number 2	1,1255	2,4614	V_LL	Serial number 2	1,1292	2,3705
W_LL	Serial number 2	1,1218	2,4859	W_LL	Serial number 2	1,1231	2,3728
U_UL	Serial number 3	1,1224	2,0074	U_UL	Serial number 3	1,1407	1,9129
V_UL	Serial number 3	1,1171	2,0032	V_UL	Serial number 3	1,1189	1,8473
W_UL	Serial number 3	1,1124	2,0081	W_UL	Serial number 3	1,1413	1,8786
U_LL	Serial number 3	1,1234	2,4373	U_LL	Serial number 3	1,1193	2,3981
V_LL	Serial number 3	1,115	2,4621	V_LL	Serial number 3	1,1302	2,4398
W_LL	Serial number 3	1,1141	2,4687	W_LL	Serial number 3	1,1523	2,4363
U_UL	Serial number 4	1,1238	2,0217	U_UL	Serial number 4	1,1181	1,9565
V_UL	Serial number 4	1,1231	2,0347	V_UL	Serial number 4	1,1188	1,9540
W_UL	Serial number 4	1,1252	2,0393	W_UL	Serial number 4	1,1287	1,9605
U_LL	Serial number 4	1,1156	2,4375	U_LL	Serial number 4	1,1146	2,4351
V_LL	Serial number 4	1,107	2,4190	V_LL	Serial number 4	1,1101	2,4467
W_LL	Serial number 4	1,099	2,4737	W_LL	Serial number 4	1,1124	2,4426
U_UL	Serial number 5	1,1135	2,0139	U_UL	Serial number 5	1,0117	2,2439
V_UL	Serial number 5	Missing	Missing	V_UL	Serial number 5	1,1188	1,9787
W_UL	Serial number 5	1,1168	1,9799	W_UL	Serial number 5	1,1124	1,9849
U_LL	Serial number 5	1,1129	2,4718	U_LL	Serial number 5	1,1156	2,4149
V_LL	Serial number 5	1,121	2,4404	V_LL	Serial number 5	1,1158	2,3894
W_LL	Serial number 5	1,121	2,4872	W_LL	Serial number 5	1,1083	2,4237
U_UL	Serial number 6	1,1254	1,9866	U_UL	Serial number 6	1,1249	2,0299
V_UL	Serial number 6	Missing	Missing	V_UL	Serial number 6	1,1364	1,9247
W_UL	Serial number 6	1,1162	1,9909	W_UL	Serial number 6	1,1146	1,9270
U_LL	Serial number 6	1,1069	2,4777	U_LL	Serial number 6	1,1225	2,4492
V_LL	Serial number 6	1,1139	2,4990	V_LL	Serial number 6	1,1189	2,5464
W_LL	Serial number 6	1,1081	2,4547	W_LL	Serial number 6	1,1141	2,5616
				U_UL	Serial number 7	1,1223	1,9932
				V_UL	Serial number 7	1,1284	2,0066
				W_UL	Serial number 7	1,1098	2,0417
				U_LL	Serial number 7	1,1234	2,4358
				V_LL	Serial number 7	1,1231	2,4449
				W_LL	Serial number 7	1,1177	2,4774
				U_UL	Serial number 8	1,1278	1,9545
				V_UL	Serial number 8	1,1234	1,9261
				W_UL	Serial number 8	1,1332	1,9424
				U_LL	Serial number 8	1,1242	2,5433
				V_LL	Serial number 8	Missing	Missing

				W_LL	Serial number 8	1,1146	2,5165

Appendix 4 – FWD V_{ce0} and R_{ce0} measurement

Passed module				Failed module			
Branch	**Serial number**	**IGBT Vce0 [V]**	**IGBT Rce0 [mΩ]**	**Branch**	**Serial number**	**IGBT Vce0 [V]**	**IGBT Rce0 [mΩ]**
U_UL	Serial number 1	1,09	1,3636	U_UL	Serial number 1	1,08	1,2949
V_UL	Serial number 1	1,0988	1,3080	V_UL	Serial number 1	1,1388	1,4173
W_UL	Serial number 1	1,085	1,3208	W_UL	Serial number 1	1,076	1,3524
U_LL	Serial number 1	1,0722	1,8678	U_LL	Serial number 1	1,097	2,0135
V_LL	Serial number 1	1,0611	1,9033	V_LL	Serial number 1	1,0787	1,9207
W_LL	Serial number 1	1,0705	1,9040	W_LL	Serial number 1	Missing	Missing
U_UL	Serial number 2	1,0946	1,3770	U_UL	Serial number 2	1,0822	1,3411
V_UL	Serial number 2	Missing	Missing	V_UL	Serial number 2	1,1287	1,4332
W_UL	Serial number 2	Missing	0,0000	W_UL	Serial number 2	1,127	1,4300
U_LL	Serial number 2	1,0883	1,9524	U_LL	Serial number 2	Missing	Missing
V_LL	Serial number 2	1,0908	1,9485	V_LL	Serial number 2	1,0761	1,8958
W_LL	Serial number 2	1,0897	1,9595	W_LL	Serial number 2	1,1023	2,0033
U_UL	Serial number 3	1,0865	1,3539	U_UL	Serial number 3	1,0794	1,3118
V_UL	Serial number 3	1,0871	1,3370	V_UL	Serial number 3	1,0754	1,2522
W_UL	Serial number 3	1,0863	1,3345	W_UL	Serial number 3	1,1359	1,3642
U_LL	Serial number 3	1,0905	1,9689	U_LL	Serial number 3	1,0759	1,8968
V_LL	Serial number 3	1,0911	1,9613	V_LL	Serial number 3	1,0792	1,9726
W_LL	Serial number 3	1,0892	1,9658	W_LL	Serial number 3	1,0797	1,9688
U_UL	Serial number 4	1,0546	1,5385	U_UL	Serial number 4	1,0896	1,3420
V_UL	Serial number 4	1,0882	1,3915	V_UL	Serial number 4	1,0864	1,3119
W_UL	Serial number 4	1,0465	1,5605	W_UL	Serial number 4	1,086	1,2783
U_LL	Serial number 4	1,0966	1,9909	U_LL	Serial number 4	1,0936	1,9496
V_LL	Serial number 4	1,0969	1,9661	V_LL	Serial number 4	1,1286	2,0696
W_LL	Serial number 4	1,0958	1,9749	W_LL	Serial number 4	1,1326	2,0353
U_UL	Serial number 5	1,0893	1,3803	U_UL	Serial number 5	1,0911	1,4211
V_UL	Serial number 5	Missing	Missing	V_UL	Serial number 5	1,0945	1,3788
W_UL	Serial number 5	1,0885	1,3798	W_UL	Serial number 5	1,0883	1,3696
U_LL	Serial number 5	1,0965	1,9801	U_LL	Serial number 5	1,09	1,9197
V_LL	Serial number 5	1,09	1,9585	V_LL	Serial number 5	1,1731	1,9442
W_LL	Serial number 5	1,0964	1,9805	W_LL	Serial number 5	1,1326	2,0276
U_UL	Serial number 6	1,0958	1,3685	U_UL	Serial number 6	1,0783	1,3524
V_UL	Serial number 6	Missing	Missing	V_UL	Serial number 6	1,1294	1,3894
W_UL	Serial number 6	1,0946	1,3271	W_UL	Serial number 6	1,066	1,2211
U_LL	Serial number 6	1,095	1,9627	U_LL	Serial number 6	1,0831	1,9194
V_LL	Serial number 6	1,0888	1,9839	V_LL	Serial number 6	1,0816	2,0015
W_LL	Serial number 6	1,095	1,9575	W_LL	Serial number 6	1,0844	1,9926
				U_UL	Serial number 7	1,0829	1,3570
				V_UL	Serial number 7	1,1314	1,4773
				W_UL	Serial number 7	1,0797	1,3519
				U_LL	Serial number 7	1,0857	1,9209
				V_LL	Serial number 7	1,0811	1,9357
				W_LL	Serial number 7	1,0881	1,9438
				U_UL	Serial number 8	1,1371	1,4134
				V_UL	Serial number 8	1,0705	1,2484
				W_UL	Serial number 8	1,1189	1,4058
				U_LL	Serial number 8	1,0878	2,0246
				V_LL	Serial number 8	1,0868	2,0186

				W_LL	Serial number 8	1,0802	1,9384

Appendix 5 – IGBT/FWD collector current i_i

Passed module				Branch	Failed Module		
Branch	**Serial number**	**IGBT i_i [A]**	**FWD i_i [A]**		**Serial number**	**IGBT i_i [A]**	**FWD i_i [A]**
U_UL	Serial number 1	495,61	489,62	U_UL	Serial number 1	507,32	537,92
V_UL	Serial number 1	501,42	502,41	V_UL	Serial number 1	492,68	447,10
W_UL	Serial number 1	502,97	507,96	W_UL	Serial number 1	Missing	514,99
U_LL	Serial number 1	501,44	504,08	U_LL	Serial number 1	498,77	483,56
V_LL	Serial number 1	505,49	500,52	V_LL	Serial number 1	501,23	516,44
W_LL	Serial number 1	493,07	495,39	W_LL	Serial number 1	Missing	Missing
U_UL	Serial number 2	Missing	Missing	U_UL	Serial number 2	496,45	544,20
V_UL	Serial number 2	Missing	Missing	V_UL	Serial number 2	504,78	476,78
W_UL	Serial number 2	Missing	Missing	W_UL	Serial number 2	498,77	479,01
U_LL	Serial number 2	506,09	500,94	U_LL	Serial number 2	Missing	Missing
V_LL	Serial number 2	498,67	500,66	V_LL	Serial number 2	498,96	520,51
W_LL	Serial number 2	495,25	498,40	W_LL	Serial number 2	501,04	479,49
U_UL	Serial number 3	497,17	495,60	U_UL	Serial number 3	487,43	511,17
V_UL	Serial number 3	500,85	501,44	V_UL	Serial number 3	516,55	538,71
W_UL	Serial number 3	501,98	502,97	W_UL	Serial number 3	496,03	450,12
U_LL	Serial number 3	501,42	498,97	U_LL	Serial number 3	511,59	514,06
V_LL	Serial number 3	499,77	500,60	V_LL	Serial number 3	498,38	492,63
W_LL	Serial number 3	498,81	500,43	W_LL	Serial number 3	490,03	493,31
U_UL	Serial number 4	502,64	491,32	U_UL	Serial number 4	502,05	486,44
V_UL	Serial number 4	499,76	519,09	V_UL	Serial number 4	501,90	500,05
W_UL	Serial number 4	497,60	489,59	W_UL	Serial number 4	496,84	513,51
U_LL	Serial number 4	497,74	496,50	U_LL	Serial number 4	500,39	529,70
V_LL	Serial number 4	505,09	502,59	V_LL	Serial number 4	501,26	482,06
W_LL	Serial number 4	497,17	500,92	W_LL	Serial number 4	500,32	488,24
U_UL	Serial number 5	496,57	499,62	U_UL	Serial number 5	491,60	489,00
V_UL	Serial number 5	Missing	500,00	V_UL	Serial number 5	503,38	501,55
W_UL	Serial number 5	503,43	500,38	W_UL	Serial number 5	505,02	509,46
U_LL	Serial number 5	501,08	497,09	U_LL	Serial number 5	497,86	532,94
V_LL	Serial number 5	504,20	505,89	V_LL	Serial number 5	503,08	483,48
W_LL	Serial number 5	494,72	497,02	W_LL	Serial number 5	499,06	483,58
U_UL	Serial number 6	498,23	491,88	U_UL	Serial number 6	482,81	495,53
V_UL	Serial number 6	Missing	Missing	V_UL	Serial number 6	503,24	445,56
W_UL	Serial number 6	501,77	508,12	W_UL	Serial number 6	513,95	558,91
U_LL	Serial number 6	500,96	500,30	U_LL	Serial number 6	512,45	513,26
V_LL	Serial number 6	493,88	498,07	V_LL	Serial number 6	494,31	492,97
W_LL	Serial number 6	505,16	501,63	W_LL	Serial number 6	493,24	493,77
				U_UL	Serial number 7	504,09	523,70
				V_UL	Serial number 7	497,67	448,25
				W_UL	Serial number 7	498,24	528,05
				U_LL	Serial number 7	502,63	502,87
				V_LL	Serial number 7	500,89	501,40
				W_LL	Serial number 7	496,48	495,72
				U_UL	Serial number 8	496,69	456,95
				V_UL	Serial number 8	506,29	570,68
				W_UL	Serial number 8	497,02	472,37
				U_LL	Serial number 8	495,45	490,77
				V_LL	Serial number 8	Missing	492,71
				W_LL	Serial number 8	504,55	516,51

Appendix 6 – IGBT/FWD conduction power loss

Passed module			Branch	Failed module		
Serial number	**IGBT conduction power loss [W]**	**FWD conduction power loss [W]**		**Serial number**	**IGBT conduction power loss [W]**	**FWD conduction power loss [W]**
Serial number 1	196,95	18,15	U_UL	Serial number 1	205,46	21,70
Serial number 1	201,17	19,16	V_UL	Serial number 1	195,03	15,49
Serial number 1	203,35	19,46	W_UL	Serial number 1	Missing	20,01
Serial number 1	221,10	20,67	U_LL	Serial number 1	215,69	19,52
Serial number 1	223,41	20,30	V_LL	Serial number 1	217,68	22,10
Serial number 1	213,62	19,96	W_LL	Serial number 1	Missing	Missing
Serial number 2	Missing	Missing	U_UL	Serial number 2	197,92	22,51
Serial number 2	Missing	Missing	V_UL	Serial number 2	204,56	17,81
Serial number 2	Missing	Missing	W_UL	Serial number 2	199,66	17,96
Serial number 2	224,97	20,86	U_LL	Serial number 2	Missing	Missing
Serial number 2	218,07	20,86	V_LL	Serial number 2	215,45	22,36
Serial number 2	214,80	20,66	W_LL	Serial number 2	217,09	19,18
Serial number 3	199,57	18,58	U_UL	Serial number 3	188,98	19,61
Serial number 3	202,40	19,01	V_UL	Serial number 3	211,67	21,59
Serial number 3	203,14	19,12	W_UL	Serial number 3	195,93	15,59
Serial number 3	219,94	20,76	U_LL	Serial number 3	229,11	21,75
Serial number 3	218,11	20,90	V_LL	Serial number 3	217,49	20,02
Serial number 3	217,20	20,87	W_LL	Serial number 3	210,78	20,08
Serial number 4	205,61	18,34	U_UL	Serial number 4	201,92	17,85
Serial number 4	203,19	20,66	V_UL	Serial number 4	201,76	18,81
Serial number 4	201,47	18,15	W_UL	Serial number 4	198,26	19,79
Serial number 4	215,06	20,67	U_LL	Serial number 4	217,74	23,71
Serial number 4	221,37	21,18	V_LL	Serial number 4	218,60	19,94
Serial number 4	213,89	21,03	W_LL	Serial number 4	217,69	20,49
Serial number 5	198,22	19,03	U_UL	Serial number 5	190,22	18,30
Serial number 5	Missing	Missing	V_UL	Serial number 5	204,13	19,25
Serial number 5	204,00	19,08	W_UL	Serial number 5	205,23	19,79
Serial number 5	219,66	20,69	U_LL	Serial number 5	214,37	23,86
Serial number 5	222,84	21,37	V_LL	Serial number 5	219,07	20,31
Serial number 5	214,18	20,69	W_LL	Serial number 5	215,15	20,02
Serial number 6	200,17	18,45	U_UL	Serial number 6	186,81	18,46
Serial number 6	Missing	Missing	V_UL	Serial number 6	203,97	15,21
Serial number 6	202,73	19,63	W_UL	Serial number 6	211,92	22,98
Serial number 6	219,06	20,92	U_LL	Serial number 6	232,51	21,85
Serial number 6	212,90	20,69	V_LL	Serial number 6	215,61	20,17
Serial number 6	222,95	21,04	W_LL	Serial number 6	214,44	20,25
			U_UL	Serial number 7	205,78	20,85
			V_UL	Serial number 7	200,71	15,62
			W_UL	Serial number 7	200,44	21,15
			U_LL	Serial number 7	221,21	20,91
			V_LL	Serial number 7	219,61	20,76
			W_LL	Serial number 7	215,39	20,34
			U_UL	Serial number 8	197,79	16,25
			V_UL	Serial number 8	205,47	24,17
			W_UL	Serial number 8	198,27	17,26
			U_LL	Serial number 8	217,36	20,11

			V_LL	Serial number 8	#DIV/0!	20,26
			W_LL	Serial number 8	225,39	22,18

Appendix 7 – IGBT/FWD switching power loss

Passed module			Branch	Failed module		
Serial number	**IGBT switching power loss [W]**	**FWD switching power loss [W]**		**Serial number**	**IGBT switching power loss [W]**	**FWD switching power loss [W]**
Serial number 1	205,46	64,64	U_UL	Serial number 1	214,08	76,08
Serial number 1	209,73	67,67	V_UL	Serial number 1	203,29	54,57
Serial number 1	210,87	68,98	W_UL	Serial number 1	Missing	70,65
Serial number 1	209,74	68,06	U_LL	Serial number 1	207,78	63,20
Serial number 1	212,73	67,22	V_LL	Serial number 1	209,59	70,99
Serial number 1	203,58	66,01	W_LL	Serial number 1	Missing	Missing
Serial number 2	Missing	Missing	U_UL	Serial number 2	206,07	77,56
Serial number 2	Missing	Missing	V_UL	Serial number 2	212,21	61,60
Serial number 2	Missing	Missing	W_UL	Serial number 2	207,78	62,13
Serial number 2	213,17	67,32	U_LL	Serial number 2	Missing	Missing
Serial number 2	207,70	67,25	V_LL	Serial number 2	207,92	71,95
Serial number 2	205,19	66,72	W_LL	Serial number 2	209,46	62,24
Serial number 3	206,60	66,05	U_UL	Serial number 3	199,42	69,74
Serial number 3	209,31	67,44	V_UL	Serial number 3	220,87	76,26
Serial number 3	210,14	67,80	W_UL	Serial number 3	205,76	55,28
Serial number 3	209,73	66,85	U_LL	Serial number 3	217,22	70,43
Serial number 3	208,52	67,24	V_LL	Serial number 3	207,49	65,35
Serial number 3	207,81	67,20	W_LL	Serial number 3	201,35	65,51
Serial number 4	210,63	65,04	U_UL	Serial number 4	210,20	63,89
Serial number 4	208,51	71,62	V_UL	Serial number 4	210,09	67,11
Serial number 4	206,92	64,63	W_UL	Serial number 4	206,36	70,30
Serial number 4	207,02	66,27	U_LL	Serial number 4	208,98	74,13
Serial number 4	212,44	67,71	V_LL	Serial number 4	209,61	62,85
Serial number 4	206,60	67,31	W_LL	Serial number 4	208,92	64,31
Serial number 5	206,16	67,01	U_UL	Serial number 5	202,50	64,49
Serial number 5	Missing	67,10	V_UL	Serial number 5	211,17	67,46
Serial number 5	211,21	67,19	W_UL	Serial number 5	212,38	69,34
Serial number 5	209,48	66,41	U_LL	Serial number 5	207,11	74,90
Serial number 5	211,78	68,49	V_LL	Serial number 5	210,95	63,19
Serial number 5	204,79	66,39	W_LL	Serial number 5	207,99	63,21
Serial number 6	207,38	65,17	U_UL	Serial number 6	196,02	66,04
Serial number 6	Missing	Missing	V_UL	Serial number 6	211,07	54,20
Serial number 6	209,99	69,02	W_UL	Serial number 6	218,96	81,05
Serial number 6	209,39	67,17	U_LL	Serial number 6	217,86	70,24
Serial number 6	204,18	66,64	V_LL	Serial number 6	204,49	65,43
Serial number 6	212,49	67,48	W_LL	Serial number 6	203,71	65,62
			U_UL	Serial number 7	211,70	72,71
			V_UL	Serial number 7	206,97	54,84
			W_UL	Serial number 7	207,39	73,74
			U_LL	Serial number 7	210,62	67,78
			V_LL	Serial number 7	209,34	67,43
			W_LL	Serial number 7	206,10	66,08
			U_UL	Serial number 8	206,25	56,90
			V_UL	Serial number 8	213,32	83,83
			W_UL	Serial number 8	206,49	60,55

			U_LL	Serial number 8	205,33	64,91
			V_LL	Serial number 8	Missing	65,37
			W_LL	Serial number 8	212,04	71,01

Appendix 8 – IGBT/FWD overall power loss

Passed module			Branch	Failed module		
Serial number	**IGBT power loss [W]**	**FWD Power loss [W]**		**Serial number**	**IGBT power loss [W]**	**FWD power loss [W]**
Serial number 1	402,40	82,79	U_UL	Serial number 1	419,53	97,78
Serial number 1	410,90	86,83	V_UL	Serial number 1	398,32	70,06
Serial number 1	414,22	88,44	W_UL	Serial number 1	Missing	90,66
Serial number 1	430,84	88,74	U_LL	Serial number 1	423,47	82,72
Serial number 1	436,14	87,52	V_LL	Serial number 1	427,27	93,09
Serial number 1	417,20	85,97	W_LL	Serial number 1	Missing	Missing
Serial number 2	Missing	Missing	U_UL	Serial number 2	404,00	100,08
Serial number 2	Missing	Missing	V_UL	Serial number 2	416,76	79,41
Serial number 2	Missing	Missing	W_UL	Serial number 2	407,44	80,09
Serial number 2	438,14	88,18	U_LL	Serial number 2	Missing	Missing
Serial number 2	425,77	88,11	V_LL	Serial number 2	423,37	94,31
Serial number 2	419,99	87,38	W_LL	Serial number 2	426,54	81,42
Serial number 3	406,17	84,64	U_UL	Serial number 3	388,40	89,36
Serial number 3	411,71	86,45	V_UL	Serial number 3	432,54	97,86
Serial number 3	413,28	86,92	W_UL	Serial number 3	401,69	70,87
Serial number 3	429,68	87,61	U_LL	Serial number 3	446,33	92,18
Serial number 3	426,63	88,13	V_LL	Serial number 3	424,99	85,37
Serial number 3	425,00	88,07	W_LL	Serial number 3	412,13	85,59
Serial number 4	416,24	83,38	U_UL	Serial number 4	412,12	81,74
Serial number 4	411,70	92,28	V_UL	Serial number 4	411,85	85,92
Serial number 4	408,39	82,78	W_UL	Serial number 4	404,62	90,08
Serial number 4	422,09	86,94	U_LL	Serial number 4	426,71	97,84
Serial number 4	433,81	88,89	V_LL	Serial number 4	428,22	82,78
Serial number 4	420,49	88,34	W_LL	Serial number 4	426,61	84,80
Serial number 5	404,38	86,03	U_UL	Serial number 5	392,72	82,79
Serial number 5	Missing	Missing	V_UL	Serial number 5	415,30	86,71
Serial number 5	415,21	86,26	W_UL	Serial number 5	417,61	89,12
Serial number 5	429,14	87,10	U_LL	Serial number 5	421,48	98,76
Serial number 5	434,62	89,86	V_LL	Serial number 5	430,03	83,49
Serial number 5	418,98	87,08	W_LL	Serial number 5	423,14	83,23
Serial number 6	407,56	83,62	U_UL	Serial number 6	382,83	84,50
Serial number 6	Missing	Missing	V_UL	Serial number 6	415,04	69,41
Serial number 6	412,72	88,65	W_UL	Serial number 6	430,88	104,03
Serial number 6	428,45	88,09	U_LL	Serial number 6	450,37	92,09
Serial number 6	417,08	87,33	V_LL	Serial number 6	420,10	85,60
Serial number 6	435,44	88,52	W_LL	Serial number 6	418,15	85,87
			U_UL	Serial number 7	417,48	93,56
			V_UL	Serial number 7	407,68	70,46
			W_UL	Serial number 7	407,83	94,89
			U_LL	Serial number 7	431,83	88,69
			V_LL	Serial number 7	428,95	88,19
			W_LL	Serial number 7	421,48	86,43
			U_UL	Serial number 8	404,04	73,15
			V_UL	Serial number 8	418,79	108,00
			W_UL	Serial number 8	404,76	77,81
			U_LL	Serial number 8	422,69	85,02

			V_LL	Serial number 8	Missing	85,63
			W_LL	Serial number 8	437,43	93,19

Appendix 9 – IGBT calculated junction temperatures

Passed module			Failed module		
Branch	**Serial number**	**IGBT Tj [°C]**	**Branch**	**Serial number**	**IGBT Tj [°C]**
U_UL	Serial number 1	130,90	U_UL	Serial number 1	134,81
V_UL	Serial number 1	132,58	V_UL	Serial number 1	129,27
W_UL	Serial number 1	133,24	W_UL	Serial number 1	Missing
U_LL	Serial number 1	135,93	U_LL	Serial number 1	134,29
V_LL	Serial number 1	136,69	V_LL	Serial number 1	135,69
W_LL	Serial number 1	133,53	W_LL	Serial number 1	Missing
U_UL	Serial number 2	Missing	U_UL	Serial number 2	132,49
V_UL	Serial number 2	Missing	V_UL	Serial number 2	132,95
W_UL	Serial number 2	Missing	W_UL	Serial number 2	131,51
U_LL	Serial number 2	137,06	U_LL	Serial number 2	Missing
V_LL	Serial number 2	135,07	V_LL	Serial number 2	135,16
W_LL	Serial number 2	134,09	W_LL	Serial number 2	134,68
U_UL	Serial number 3	131,65	U_UL	Serial number 3	129,16
V_UL	Serial number 3	132,68	V_UL	Serial number 3	136,91
W_UL	Serial number 3	132,97	W_UL	Serial number 3	129,88
U_LL	Serial number 3	135,66	U_LL	Serial number 3	138,69
V_LL	Serial number 3	135,21	V_LL	Serial number 3	134,73
W_LL	Serial number 3	134,94	W_LL	Serial number 3	132,68
U_UL	Serial number 4	133,17	U_UL	Serial number 4	132,39
V_UL	Serial number 4	133,13	V_UL	Serial number 4	132,66
W_UL	Serial number 4	131,87	W_UL	Serial number 4	131,82
U_LL	Serial number 4	134,39	U_LL	Serial number 4	135,97
V_LL	Serial number 4	136,42	V_LL	Serial number 4	135,05
W_LL	Serial number 4	134,24	W_LL	Serial number 4	134,95
U_UL	Serial number 5	131,47	U_UL	Serial number 5	129,35
V_UL	Serial number 5	Missing	V_UL	Serial number 5	133,28
W_UL	Serial number 5	133,23	W_UL	Serial number 5	133,84
U_LL	Serial number 5	135,54	U_LL	Serial number 5	135,20
V_LL	Serial number 5	136,63	V_LL	Serial number 5	135,40
W_LL	Serial number 5	133,90	W_LL	Serial number 5	134,27
U_UL	Serial number 6	131,80	U_UL	Serial number 6	127,89
V_UL	Serial number 6	Missing	V_UL	Serial number 6	131,91
W_UL	Serial number 6	133,01	W_UL	Serial number 6	137,12
U_LL	Serial number 6	135,50	U_LL	Serial number 6	139,33
V_LL	Serial number 6	133,61	V_LL	Serial number 6	133,97
W_LL	Serial number 6	136,66	W_LL	Serial number 6	133,67
			U_UL	Serial number 7	134,16
			V_UL	Serial number 7	130,81
			W_UL	Serial number 7	132,71
			U_LL	Serial number 7	136,09
			V_LL	Serial number 7	135,59
			W_LL	Serial number 7	134,25
			U_UL	Serial number 8	130,43
			V_UL	Serial number 8	135,48
			W_UL	Serial number 8	130,90
			U_LL	Serial number 8	134,34
			V_LL	Serial number 8	Missing
			W_LL	Serial number 8	137,34

Appendix 10 – FWD calculated junction temperatures

Passed modules			Failed modules		
Branch	**Serial number**	**FWD Tj [°C)**	**Branch**	**Serial number**	**FWD Tj [°C]**
U_UL	Serial number 1	105,51	U_UL	Serial number 1	109,48
V_UL	Serial number 1	106,88	V_UL	Serial number 1	102,92
W_UL	Serial number 1	107,42	W_UL	Serial number 1	Missing
U_LL	Serial number 1	108,66	U_LL	Serial number 1	107,00
V_LL	Serial number 1	108,85	V_LL	Serial number 1	109,12
W_LL	Serial number 1	107,12	W_LL	Serial number 1	Missing
U_UL	Serial number 2	Missing	U_UL	Serial number 2	108,67
V_UL	Serial number 2	Missing	V_UL	Serial number 2	105,98
W_UL	Serial number 2	Missing	W_UL	Serial number 2	105,38
U_LL	Serial number 2	109,09	U_LL	Serial number 2	Missing
V_LL	Serial number 2	108,13	V_LL	Serial number 2	109,04
W_LL	Serial number 2	107,56	W_LL	Serial number 2	107,01
U_UL	Serial number 3	106,13	U_UL	Serial number 3	105,61
V_UL	Serial number 3	106,88	V_UL	Serial number 3	110,50
W_UL	Serial number 3	107,08	W_UL	Serial number 3	103,33
U_LL	Serial number 3	108,34	U_LL	Serial number 3	110,43
V_LL	Serial number 3	108,19	V_LL	Serial number 3	107,60
W_LL	Serial number 3	108,06	W_LL	Serial number 3	106,65
U_UL	Serial number 4	106,68	U_UL	Serial number 4	106,08
V_UL	Serial number 4	107,88	V_UL	Serial number 4	106,80
W_UL	Serial number 4	105,97	W_UL	Serial number 4	106,98
U_LL	Serial number 4	107,63	U_LL	Serial number 4	109,87
V_LL	Serial number 4	108,87	V_LL	Serial number 4	107,34
W_LL	Serial number 4	107,75	W_LL	Serial number 4	107,57
U_UL	Serial number 5	106,23	U_UL	Serial number 5	104,76
V_UL	Serial number 5	Missing	V_UL	Serial number 5	107,18
W_UL	Serial number 5	107,10	W_UL	Serial number 5	107,79
U_LL	Serial number 5	108,20	U_LL	Serial number 5	109,64
V_LL	Serial number 5	109,11	V_LL	Serial number 5	107,59
W_LL	Serial number 5	107,42	W_LL	Serial number 5	107,03
U_UL	Serial number 6	106,05	U_UL	Serial number 6	104,32
V_UL	Serial number 6	Missing	V_UL	Serial number 6	104,10
W_UL	Serial number 6	107,33	W_UL	Serial number 6	111,47
U_LL	Serial number 6	108,32	U_LL	Serial number 6	110,72
V_LL	Serial number 6	107,32	V_LL	Serial number 6	107,26
W_LL	Serial number 6	108,93	W_LL	Serial number 6	107,15
			U_UL	Serial number 7	108,56
			V_UL	Serial number 7	103,70
			W_UL	Serial number 7	108,06
			U_LL	Serial number 7	108,70

			V_LL	Serial number 7	108,39
			W_LL	Serial number 7	107,51
			U_UL	Serial number 8	103,90
			V_UL	Serial number 8	111,23
			W_UL	Serial number 8	104,79
			U_LL	Serial number 8	107,35
			V_LL	Serial number 8	Missing
			W_LL	Serial number 8	109,91

Appendix 11 – J-type thermocouples locations and names

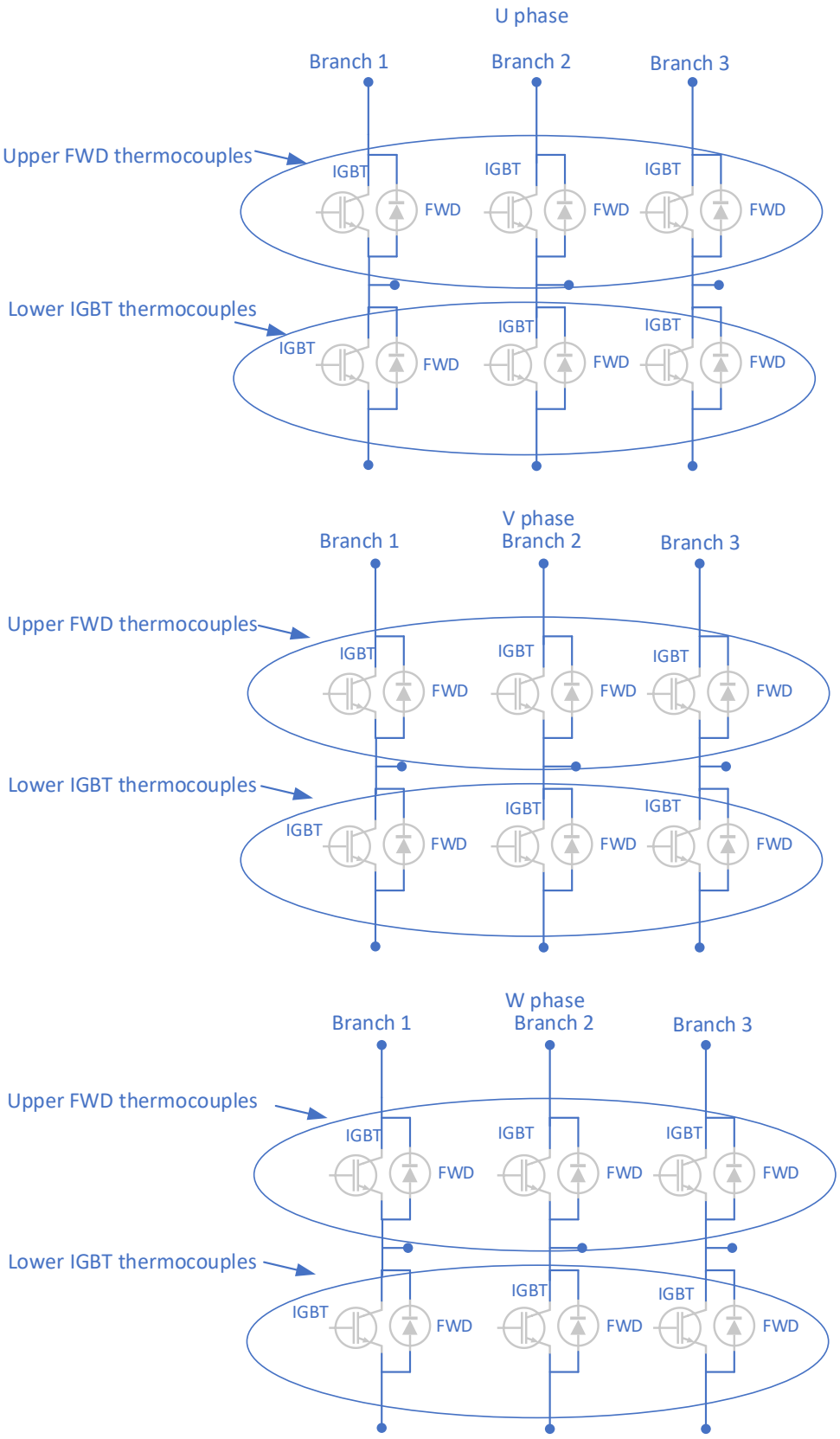

Label	Description of J-type thermocouple location
LC1_U_L2_I	Inverter unit LC1 U phase lower IGBT second branch
LC1_U_L3_I	Inverter unit LC1 U phase lower IGBT third branch
LC1_U_U3_D	Inverter unit LC1 U phase upper FWD third branch
LC1_V_L2_I	Inverter unit LC1 V phase lower IGBT second branch
LC1_V_L3_I	Inverter unit LC1 V phase lower IGBT third branch
LC1_V_U3_D	Inverter unit LC1 V phase upper FWD third branch
LC1_W_L2_I	Inverter unit LC1 W phase lower IGBT second branch
LC1_W_L3_I	Inverter unit LC1 W phase lower IGBT third branch
LC1_W_U3_D	Inverter unit LC1 W phase upper FWD third branch
LC2_U_L1_I	Inverter unit LC2 U phase lower IGBT first branch
LC2_U_L2_I	Inverter unit LC2 U phase lower IGBT second branch
LC2_U_L3_I	Inverter unit LC2 U phase lower IGBT third branch
LC2_U_U1_D	Inverter unit LC2 U phase upper FWD first branch
LC2_U_U2_D	Inverter unit LC2 U phase upper FWD second branch
LC2_U_U3_D	Inverter unit LC2 U phase upper FWD third branch
LC2_V_L1_I	Inverter unit LC2 V phase lower IGBT first branch
LC2_V_L2_I	Inverter unit LC2 V phase lower IGBT second branch
LC2_V_L3_I	Inverter unit LC2 V phase lower IGBT third branch
LC2_V_U1_D	Inverter unit LC2 V phase upper FWD first branch
LC2_V_U2_D	Inverter unit LC2 V phase upper FWD second branch
LC2_V_U3_D	Inverter unit LC2 V phase upper FWD third branch
LC2_W_L1_I	Inverter unit LC2 W phase lower IGBT first branch
LC2_W_L2_I	Inverter unit LC2 W phase lower IGBT second branch
LC2_W_L3_I	Inverter unit LC2 W phase lower IGBT third branch
LC2_W_U1_D	Inverter unit LC2 W phase upper FWD first branch
LC2_W_U2_D	Inverter unit LC2 W phase upper FWD second branch
LC2_W_U3_D	Inverter unit LC2 W phase upper FWD third branch

Appendix 12 – Temperatures from thermocouples and calculated lifecycles

Label	Cycles [thousand]	Operation time [h]	min1 [°C)	max1 [°C)	min2 [°C)	max2 [°C)
LC1_U_L2_I	649	21633,3	56	87	56	82
LC1_U_L3_I	185	6166,7	56	98	55	88
LC1_U_U3_D	439	14633,3	56	87	55	87
LC1_V_L2_I	418	13933,3	56	91	56	85
LC1_V_L3_I	127	4233,3	56	103	56	90
LC1_V_U3_D	254	8466,7	56	93	56	91
LC1_W_L2_I	940	31333,3	56	86	56	80
LC1_W_L3_I	242	8066,7	56	96	56	85
LC1_W_U3_D	335	11166,7	56	91	56	89
LC2_U_L1_I	590	19666,7	56,81	89,48	56,78	82,12
LC2_U_L2_I	382	12733,3	56,89	92,37	56,88	85,86
LC2_U_L3_I	76	2533,3	56,65	108,13	56,62	96,53
LC2_U_U1_D	2155	71833,3	56,23	78,45	56,18	78,76
LC2_U_U2_D	1240	41333,3	56,20	80,97	56,14	82,00
LC2_U_U3_D	196	6533,3	56,23	94,65	56,17	94,01
LC2_V_L1_I	509	16966,7	56,61	90,22	56,60	83,24
LC2_V_L2_I	352	11733,3	56,64	93,17	56,63	85,40
LC2_V_L3_I	125	4166,7	56,33	102,75	56,30	91,59
LC2_V_U1_D	1391	46366,7	55,94	80,58	55,88	80,69
LC2_V_U2_D	1688	56266,7	56,00	79,49	55,93	79,77
LC2_V_U3_D	218	7266,7	56,00	93,11	55,93	93,44
LC2_W_L1_I	458	15266,7	56,39	90,41	56,41	84,59
LC2_W_L2_I	315	10500	56,34	93,56	55,69	85,88
LC2_W_L3_I	103	3433,3	56,16	104,54	56,12	93,38
LC2_W_U1_D	1143	38100	55,78	81,36	55,80	81,90
LC2_W_U2_D	6940	231333,3	55,84	74,03	55,80	72,24
LC2_W_U3_D	204	6800	56,01	94,02	56,06	93,73